

# The life cycle of Large Igneous Provinces

Ben Black<sup>1†,2</sup>, Leif Karlstrom<sup>3</sup>, Tamsin A. Mather<sup>4</sup>

<sup>1</sup> Department of Earth and Planetary Science, Rutgers University, New Brunswick, NJ, USA

<sup>2</sup> Department of Earth and Atmospheric Science, CUNY City College, New York, NY, USA

<sup>3</sup> Department of Earth Sciences, University of Oregon, Eugene, OR, USA

<sup>4</sup> Department of Earth Sciences, University of Oxford, South Parks Road, Oxford, UK

email<sup>†</sup>: [bblack@eps.rutgers.edu](mailto:bblack@eps.rutgers.edu)

## Key messages

- Large Igneous Provinces (LIPs) mobilize climate-impacting gases from the solid Earth, and have been implicated in major environmental disruptions.
- Mantle melting varies between LIPs: Continental LIP main-phase melting tends to be shallower than early and late phases, whereas oceanic LIPs differ, suggesting lithosphere thickness is among the controls modulating melting.
- LIPs exhibit an evolving lithospheric transport system that links waxing and waning generation of a prodigious volume ( $10^6$ - $10^7$  km<sup>3</sup>) of mantle melt with intrusions and surface outpourings of lava.
- LIP volatiles originate from the mantle, continental lithospheric mantle, and crust. Evolving magmatic chemistry, intrusion, volatile flushing, and diffuse degassing complicate the relationship between pace of emissions (particularly CO<sub>2</sub>) and surface eruption rates.
- Understanding links between LIP melt generation, lithospheric magma plumbing, and surface climate requires high-resolution timelines for these systems combining geodynamic modelling, geochronology, and geochemical datasets.

## Editorial summary:

Major environmental disruptions throughout Earth's history are often linked to extensive magmatic events, termed Large Igneous Provinces (LIPs). This Review explores the coupled evolution of mantle melting, magmatism, and volatile release over the life cycle of LIPs.

## Abstract

Extremely voluminous magmatic systems known as Large Igneous Provinces (LIPs) punctuate Earth's history, and the gases they release plausibly link large-scale geodynamic and magmatic processes with major climate shifts in Earth's geological record. However, quantifying the relationships between magmatism, gas release, and environmental changes remains challenging. In this Review, we explore the major insights and outstanding questions regarding the linked evolution of mantle melting, expansive magmatic systems, and the redistribution of volatiles from the solid Earth to the atmosphere. The evolution of mantle melt generation during LIP episodes sets the fundamental tempo of magma emplacement throughout the crust. The progression of crustal LIP magmatism and associated hydrothermal activity help shape the chemical evolution of the continental lithosphere and surface environment. Prolonged exhalation of magmatic and metamorphic volatiles can decouple the tempo of gas release—a potential key driver of environmental changes—from the tempo of extrusive volcanic activity. LIPs demonstrate how large-scale magmatic systems interact with the surrounding lithosphere to drive evolving regimes of magma and volatile transfer through the crust. New, temporally resolved constraints on the evolution of LIP plumbing systems are needed to keep pace with increasingly precise timelines of paleoenvironmental change during LIP emplacement.

## [H1] Introduction

Large Igneous Provinces (LIPs) are among the most extensive magmatic events punctuating Earth's history. They typically emplace  $10^5 - 10^7 \text{ km}^3$  of mainly mafic magma on the Earth's surface and throughout the lithosphere. More than 24 oceanic and continental LIP events have occurred over the past 275 Myr<sup>1, 2</sup> at intervals of  $\sim 10\text{-}50 \text{ Myr}^{1, 3, 4}$ . Prominent examples include the  $\sim 16 \text{ Ma}$  Columbia River Basalts (CRB), the  $\sim 66 \text{ Ma}$  Deccan Traps, the  $\sim 110 \text{ Ma}$  Ontong-Java Plateau (OJP), and the  $\sim 252 \text{ Ma}$  Siberian Traps. Advances in geochronology, new geochemical tools, and advances in modeling of magmatic processes have opened the door to a fresh understanding of LIP magmatism and volatiles as dynamic and temporally evolving systems. Understanding the origins, evolution, and consequences of LIPs are critical to reconstructing past interactions between solid Earth reservoirs and surface environments.

In the geological record, at least four of the 'big five' severest mass extinctions [G] overlap in time with LIP events<sup>5-9</sup>. Many other LIPs are temporally associated with major carbon cycle perturbations and/or ocean anoxia events that drive more minor species overturn (less acute than the 'big five')<sup>5-9</sup>. Volatile release [G]—especially of  $\text{CO}_2$ , sulfur species and halogens—represents a potentially key causal mechanism linking LIP emplacement and major environmental changes. The large scale of LIPs, their intra-plate location, and potentially deep mantle source enable them to remobilize volatiles from the deep mantle, the stable continental lithospheric mantle (CLM) [G], and the crust<sup>10, 11</sup>.

A dynamic network of channels and storage zones links regions of LIP melt generation in the mantle with regions of magma solidification in the crust and eruption at the surface (Figure 1), forming a trans-crustal transport system [G]<sup>35, 36</sup>. These magma transport systems are exposed today as relic LIP dikes, sills, and layered intrusions, including the most extensive mafic plutonic structures on Earth<sup>12</sup>. Vast radiating and circumferential dike swarms in Precambrian exposures, such as the 1270 Ma Mackenzie LIP in Canada that spans  $>10^7 \text{ km}^2$ , reflect the scale of crustal magma transfer<sup>13, 14</sup>. The variety of LIP magma geochemistries, including tholeiitic [G] and alkaline [G] compositions, reflects the diversity of mantle melting conditions.

Continued advances in understanding the timing and extent of LIP volcanism have strengthened the temporal link with surface environmental changes. However, the mechanistic relationships between LIP activity and the progression of environmental change remain elusive. Resolving these relationships depends on developing an integrated picture of evolving processes within the LIP magma transport network, with such understanding just beginning to emerge (Figure 1).

In this Review, we discuss the life cycle of LIPs from their origin, evolution, and termination. Other reviews have focused on LIP surface extrusions or the link with mass extinctions 2, 6, 7, 9, 15, 16. Here, we address the petrology and lithospheric plumbing of LIPs, including magma storage, transport, and crustal rheology. In particular, we examine how these LIP processes facilitate volatile exchange between solid Earth and surface environments. We present a compilation of volatile inventories through LIP evolution (Supplementary Dataset 1) to capture emerging constraints on the scale of outgassing and variability amongst LIPs. We highlight future research directions that integrate petrologic, geochemical, and geophysical techniques to resolve the architecture, timescales, and consequences of LIP magmatism.

## **[H1] The origins of LIP magmatism**

In this section, the bottom-up mantle controls on the origin and evolution of LIP magmatic systems are discussed. Variability in mantle source characteristics drives evolving LIP magma supply, volatiles, and compositional evolution. Top-down processes, such as lithospheric thickening, extension, or delamination, influence mantle melting and therefore create feedbacks between mantle and lithospheric evolution.

## ***[H2] Connections to the deep mantle***

The origins of prodigious mantle melting during LIP emplacement are the subject of long-standing debate<sup>17, 18</sup>. The plume head and tail model postulates that hot, buoyant mantle plumes [G] rooted at the core-mantle boundary cause LIPs when plume heads arrive at the base of the lithosphere<sup>17, 19, 20</sup>. Alternative models include edge-driven convection [G]<sup>19</sup>, delamination [G]<sup>21</sup>, impact-induced melting<sup>22</sup>, and thermal anomalies due to changes in mantle flow or reduced mantle heat loss beneath continents<sup>23, 24</sup>.

These melting mechanisms are not mutually exclusive, and different LIPs could exhibit combinations of processes. However, seismic<sup>25</sup>, geochemical<sup>26, 27</sup>, and petrologic<sup>28-30</sup> evidence are consistent with the view that thermochemically distinct mantle plumes exist, that some plumes are rooted near the core-mantle boundary<sup>25, 31, 32</sup>, and that their arrival at the base of the lithosphere can initiate LIP melting<sup>19, 33</sup>. Mantle plumes have been proposed to incorporate recycled oceanic crust<sup>34</sup>, less degassed primordial reservoirs in the lower mantle<sup>26, 27</sup>, and perhaps even material from the core<sup>35</sup>.

## ***[H2] Mantle potential temperatures***

Mantle potential temperatures [G] 100-400 °C above the ambient mantle are a key factor in time-evolving LIP mantle melting. Elevated mantle potential temperatures have been inferred for LIPs, including the Siberian Traps, Caribbean LIP, Parana-Etendeka, and Deccan Traps<sup>28-30, 36</sup>, with more subtly elevated temperatures in the Central Atlantic Magmatic Province (CAMP)<sup>29</sup>. Higher mantle temperatures are consistent with upwelling thermochemical mantle plumes, though alternative mechanisms such as thermal insulation beneath supercontinents have also been proposed<sup>23</sup>. Regardless, anomalously hot mantle likely plays an important role in generating the tremendous volumes of mantle melt that characterize LIPs. Geodynamic modeling [G] of mantle plumes implies lateral and vertical temperature gradients within the plume head, with a hot core and cooler margins<sup>37</sup>, in line with the range in petrologically determined mantle temperatures across different magma suites<sup>38</sup>. Such temperature as well as pressure variations relative to the mantle solidus translate to variations in the degree of melting and volume of melt production.

Mantle temperatures likely evolve through time. Along with compositional and melting depth heterogeneity, the resulting changes in LIP melting and the volumes of melt generation help drive bottom-up shifts in the phase of the LIP life cycle. Mantle potential temperatures beneath ocean island basalts are typically 100-200 °C cooler than those beneath LIPs, pointing to broad secular cooling of mantle plumes on 10<sup>7</sup> year timescales<sup>29</sup>-- possibly linked to the transition from plume heads to tails<sup>19</sup>. However, geothermometry from 60 Ma to the present from the North Atlantic tracks notable fluctuations in the Iceland plume<sup>39</sup>, suggesting that increasing spatial and temporal resolution could reveal more complicated patterns of temperature evolution.

## **[H2] Composition of mantle sources**

The range of major element [G] and trace element [G] compositions in LIP magmas is inconsistent with a single mantle source composition. Instead, primary melts likely reflect varying proportions of recycled and enriched material from the deep mantle, shallow asthenospheric mantle similar to the source of mid-ocean ridge basalts, CLM, and in some cases interactions with a downgoing subducting slab<sup>34, 40-42</sup>. Trace element ratios can potentially distinguish between sources of LIP melting<sup>43</sup>. Mantle plume heterogeneity is recorded in the geochemistry of hotspot<sup>44</sup> and primitive LIP magmas<sup>45</sup>. However, magma storage and transport can homogenize trace element and isotope systematics especially in main phase basalts<sup>46</sup>, making source heterogeneity harder to distinguish.

Subducted oceanic lithosphere is rich in volatiles relative to the average mantle<sup>34, 47</sup>. Therefore, melting of subduction-derived, recycled pyroxenite-rich mantle could occur at higher pressures and deliver higher volatile concentrations than average mantle melting<sup>34, 48, 49</sup>. However, whether mantle plumes do entrain some recycled pyroxenite derived from subducted oceanic crust remains debated. Furthermore, the extent to which subducted volatiles such as carbon and sulfur remain coupled during recycling is a major outstanding question, owing to complicated redox transitions between the upper and lower mantle<sup>50</sup>. Mass-independent fractionation of sulfur isotopes has been used to detect recycled Archean sulfur<sup>51</sup> and Mg isotopes have been used to detect recycled carbonates<sup>52</sup> in the sources of ocean island basalts, implying that some sulfur and carbon do indeed remain coupled to recycled lithologies on billion-year timescales.

## **[H2] Interactions with the lithosphere**

Constraints on melting pressures come from trace element distributions sensitive to the degree of partial mantle melting [G] and presence of garnet (implying melting pressures  $\geq 3$  GPa)<sup>34, 53-56</sup>. These models leverage experimental data for melt compositions in equilibrium with mantle minerals<sup>57</sup>. Melting pressure estimates for continental LIPs -- including the Siberian Traps, Parana-Etendeka, and the North Atlantic Igneous Province (NAIP)<sup>34, 53-55</sup>-- are consistent with deep melting in the garnet stability field during the early and waning phases of LIPs (Figure 2), including some alkaline and ultramafic magmas that originate from depths as great as ~6-8 GPa (~180-240 km)<sup>54, 55, 58</sup>. In contrast, during the main phase of continental LIPs, melting shallows into the spinel stability field, and main phase tholeiitic lavas from oceanic and continental LIPs originate at relatively shallow pressures of 1.5-4 GPa (~45-120 km)<sup>54, 56, 59</sup>.

Leading explanations for progression from deeper to shallower LIP melting involve CLM thinning through extension facilitated by thermal weakening of the lithosphere or delamination of dense pyroxene-garnet intrusions at the base of the lithosphere<sup>21, 34, 60</sup>. Decreasing melting depth through the course of continental LIP magmatism implies disruption of the CLM. Alkaline, sometimes ultra-potassic, dikes and lavas originating from low-degree (1-3 %) melting of the CLM<sup>54, 61, 62</sup> are one byproduct of this lithosphere disruption (Figure 1).

Evolution from deep to shallow melting is not evident in oceanic LIPs, possibly owing to the absence of thick lithosphere in oceanic settings. Thick lithosphere in some continental settings can stall basaltic melts at sufficient depths that they freeze as dense, delamination-prone eclogites. Indeed, there is evidence for a progression from shallow to deep melting in some oceanic LIPs. For example, trace element data from OJP and Kerguelen basalts hint at progressively decreasing

degrees of melting <sup>63-65</sup>, perhaps caused by magmatic thickening of the lithosphere or a waning plume.

## **[H1] Upper mantle to surface structure**

LIP magmas are transported through, stored, and stalled in the lithosphere, which has consequences for deformation and hydrothermal activity in the crust.

## **[H2] Magmatic plumbing system**

The mechanisms of melt transfer from asthenospheric melting zones to the base of the lithosphere are among the most poorly constrained aspects of the LIP **magma plumbing system** [G]. At mid-ocean ridge settings <sup>66</sup>, two-phase reactive compacting flow models suggest that initial grain-boundary melts can coalesce to form reactive melt channels that efficiently transport melt upwards from melting regions <sup>67</sup>. Similar deep transport phenomena likely occur in LIPs. For both LIPs and oceanic ridges, variations in the depth of the lithosphere-asthenosphere boundary can act as an inverted catchment, focusing buoyant melts to thinner areas of the lithosphere <sup>68, 69</sup>.

Alternatively, active modification of the lower crust (including possible delamination in the case of the CRB <sup>70</sup>) and lithospheric mantle by ascending melts have been indicated by seismic constraints from receiver functions and surface wave radial anisotropy in the Deccan and CRB provinces <sup>71, 72</sup>. Large-volume magma reservoirs are preserved as reflective, high seismic velocity layers with Moho-depth cumulative thicknesses of several to >10 km beneath the Deccan Traps, Siberian Traps, Emeishan Traps, OJP, Kerguelen, CRB, and High Arctic LIP <sup>73-77</sup> (Figure 2). The extent to which these magma reservoirs were integrated versus a more complex network of stacked sills cannot be clearly resolved from available seismic data.

Rare, exhumed deep intrusions provide additional information on the structure of LIP plumbing systems. The ~580-560 Ma Seiland Igneous Province <sup>78</sup>(Northern Norway) represents a possible exposure of a deep LIP magma plumbing system in fossil form. It comprises >17,000 km<sup>3</sup> of mafic, ultramafic, alkaline, and felsic magmas that were emplaced at lower crustal pressures within gneissic meta-sedimentary and meta-igneous country rocks <sup>79</sup>. The Seiland province has been interpreted as the roots of the Ediacaran-age Central Iapetus Magmatic Province <sup>79</sup>. The high proportion (1-5%) of carbonate and sulfide assemblages in the Seiland province point to the existence and mobility of exsolved volatiles in lower crustal magma transfer stations <sup>78</sup>, supporting the view that volatiles could play a key role in modulating magma buoyancy, overpressure, and further ascent into the crust <sup>80-82</sup>.

These combined constraints are sufficient for postulating a conceptual framework for the spatial structure of LIP magma ascent (Figure 1). Deep accumulation of channelized partial melt in the mantle results in fluid overpressure<sup>85</sup>, associated either with compositional buoyancy (including deep CO<sub>2</sub> exsolution) or mass accumulation<sup>81, 83</sup> that leads to fracturing and upward dike propagation. Growth of large magma reservoirs at a neutral buoyancy region near the base of the crust<sup>46, 75</sup>(and potentially at shallower levels) is limited by structural destabilization and further dike propagation, driving continued ascent upward through the crust. Episodic re-use of transport pathways becomes more common in cool shallow crust, resulting in large composite dike and sill structures<sup>12</sup>.

## **[H2] Intrusive to Extrusive ratios**

The magmatic **Intrusive to Extrusive (I:E) ratio** [G] represents a major uncertainty for relating surface volcanism to magma supply, not just for LIPs but across different magmatic settings<sup>84-87</sup>. The I:E ratio for LIPs has been estimated between 10:1 and 1:1 based on seismic, petrologic, and gravity data, implying that most magmas do not erupt<sup>73, 75, 88</sup>.

Seismic constraints on intrusive magmas at crustal depths omit frozen magmas in the mantle lithosphere, especially magmas that produce dense eclogites that can sink into the mantle<sup>21, 34, 70</sup>. Geodynamic simulations of the Deccan Traps and the NAIP<sup>89, 90</sup> predict melt production of 4-10×10<sup>7</sup> km<sup>3</sup> during LIP emplacement. Comparison of these volumes of melt production from geodynamic modeling with Deccan and NAIP extrusive volume estimates<sup>67, 91</sup> suggests as little as 1-5% by volume of mantle melts reached the surface during the main phase of magmatism. Interestingly, these same geodynamic modeling predictions of 10<sup>7</sup>-10<sup>8</sup> km<sup>3</sup> mantle melt align well with total volume estimates for large oceanic LIPs such as Ontong-Java (~5×10<sup>7</sup> km<sup>3</sup> from ref. <sup>92</sup>), consistent with less delamination in oceanic settings.

Possible controls on magma storage depths and the balance between intrusion and eruption involve substantial interplay between magma supply rate, buoyancy (strongly influenced by volatiles), and time-evolving, temperature-dependent crustal rheology<sup>93-96</sup>. During early LIP emplacement, the middle to upper continental crust is expected to be cold and strong, favoring growth of magma chambers in the lower crust and mantle lithosphere (Figure 2). Conduction of heat from the hot plume head, advection of heat by ascending magmas, and latent heat associated with freezing of intrusions progressively alter the overall thermomechanical regime by modifying viscosity of the crust, stress state, and mechanical anisotropy<sup>97, 98</sup>. This interplay—which might also unfold similarly in rifts and arcs—likely contributes to a broadening distribution of storage



depths during the main phase of magmatism relative to other phases of the LIP life cycle (Figure 2b).

High magma supply to the lithosphere coincides with high degrees of melting. As these large volumes of hot basaltic magma transfer heat from the mantle <sup>99</sup>, a broad swath of the crust heats sufficiently to easily accommodate growing magma reservoirs <sup>100</sup>, further favoring staging in extensive crustal magma storage and transfer systems. Clinopyroxene barometry generally supports storage regions spanning the crust during the main phase of magmatism (Figure 2). However, clinopyroxene barometry skews towards shallower storage depths than indicated by high seismic velocity regions (Figure 2).

As magmas ascend into the brittle upper crust, dikes and sills become the dominant form of magma transport. Magnetic and mineral textures suggest that lateral rather than vertical magma flow becomes increasingly important at shallow depths <sup>101</sup>. Giant dike swarms facilitate lateral transfer of LIP magmas across distances of 100s-1000s km <sup>13, 102</sup>. Interconnected sills and sill-fed dikes in the Ferrar province <sup>103</sup>, or dikes in the CRB, can eventually breach the crust to feed surface flows <sup>104-106</sup>. Such lateral magma flow implies approximately neutral buoyancy <sup>107</sup>, which places an upper limit on volatile contents for a given melt composition and wall-rock density <sup>80</sup>.

## ***[H2] Rapid ascent of alkaline magmas from the mantle***

Alkaline magmas represent a small proportion of the overall volume of most LIPs because their lower degrees of melting yield smaller volumes of melt, and the geologic record of alkaline magmatism might be partially obscured by emplacement of more voluminous tholeiitic magmas. Nevertheless, alkaline rocks represent important markers for the extent and diversity of LIP melting conditions including near-solidus melting on the margins of plumes and potential disruption of the CLM <sup>11</sup>.

Some alkaline magmas appear to largely bypass the tholeiitic crustal transport network, likely due to rapid ascent fueled by high volatile contents <sup>108</sup>. Lower crustal or mantle xenoliths [G] <sup>109</sup> found in some alkaline dikes and lavas attest to fast and relatively direct ascent from the depths at which these xenoliths were entrained. Such direct routes from the mantle could mean that these rocks preserve clearer records of mantle processes than tholeiitic magmas that have experienced extensive mixing, fractionation and contamination in the crust, further motivating future investigation of the petrology and geochronology of alkaline LIP rocks.

## ***[H2] Crustal deformation and surface topography***

Interactions between mantle magma supply and the crust are recorded by time-evolving surface topography and crustal deformation. For example, classical plume models predict 1000 km-scale doming associated with mantle plume impingement on the lithosphere<sup>20</sup>. Subsequent lateral spreading and rifting associated with thermal evolution of the crust during- and post-flood basalt emplacement can determine topographic uplift and erosion patterns<sup>110</sup>. Some Phanerozoic LIPs appear to display this progression (for example, Paraná–Etendeka<sup>111</sup>). However, a consistent global LIP topographic signature is not clear<sup>118,119</sup>. Indeed, 3D thermochemical plumes rising in a realistic mantle flow field can have complex topographic consequences<sup>112-114</sup>.

Perhaps the clearest evidence for magmatically-driven **dynamic topography [G]** comes from hotspots such as Galapagos, Iceland and Yellowstone<sup>115</sup>, where uplift and subsidence exceeding the plume area has been attributed to flexure and lower crustal flow associated with magmatic loading<sup>116, 117</sup>. Although obscured by lavas in many LIPs, numerous regional subsidence and faulting structures in the CRB have onset times coincident with main phase magmatism<sup>127</sup>. Similar syn-eruptive subsidence features have been proposed in the Emeishan Traps<sup>118</sup>.

The lateral deformation associated with LIP emplacement is even more profound. Although we do not focus on rifting here, flood basalt-scale volcanism has been hypothesized to play a role in rifting events<sup>119-121</sup> and supercontinent breakup<sup>119, 122, 123</sup>. Conversely, pre-existing crustal structures and stress state clearly impact the progression of LIP magmatism, as observed in the Deccan and CRB provinces<sup>124</sup>.

## **[H2] LIP hydrothermal systems**

The crust surrounding LIP magmas—both continental and oceanic—hosts hydrothermal activity that might in some instances rival mid-ocean ridge hydrothermal systems in scale<sup>125</sup>, but LIP hydrothermal systems have received comparatively little attention. Weathering of mafic LIP rocks has been proposed as an important but controversial factor in Earth’s silicate weathering cycle<sup>126, 127</sup>. At mid-ocean ridges, hydrothermally mediated carbon sequestration in newly formed oceanic crust likely counterbalances CO<sub>2</sub> outgassing<sup>128</sup>. Oceanic LIP lavas are often pervasively altered<sup>129, 130</sup>, but how quickly this alteration takes place after emplacement is uncertain<sup>131</sup>. Improved understanding of alteration in LIP hydrothermal systems—in continental and oceanic settings—could be vital to assessing the role of LIPs in the long-term drawdown of atmospheric CO<sub>2</sub> in Earth’s past<sup>131</sup>.

Signatures of hydrothermal activity provide a powerful tool for inferring temporal progression of LIPs. For example, heat loss from CRB dikes drove fluid flow<sup>125</sup>, and the pulsed

cooling, heating and re-melting of the ~300 km<sup>3</sup> LIP-related Skaergaard intrusive complex and its host rocks are encoded in crystal to km-scale variability of oxygen isotopes<sup>132, 133</sup>.

## **[H1] The tempo and death of LIPs**

The multiscale transport and eruption tempo of LIP magmas highlights characteristic phases of the LIP life cycle. LIP stratigraphies, often comprising of hundreds of lava flows<sup>134</sup>, are generally subdivided into compositionally or stratigraphically distinct formations. In the case of the CRB (Figure 3) these have been further subdivided into members that comprise mappable units with similar geochemistry, each containing a variable number of individual eruptions<sup>135</sup>. The variations in the tempo of LIP magmatism on these different scales are now discussed.

## **[H2] Tempo at the formation scale**

Advances in the precision of U-Pb and Ar/Ar geochronology, improved consistency with magnetostratigraphy, and refinements of erupted volumes, provide increasing resolution of the pace of LIP magmatism<sup>136-143</sup>. Although there are differences between LIPs, high-precision geochronology suggests that many continental LIPs are characterized by a ‘main phase’ of tholeiitic eruptive activity spanning <1 Myr during which most of the lava volume erupts. There is notable complexity in cases such as the NAIP<sup>174</sup> and the Paraná–Etendeka<sup>144</sup> where evidence exists of marked precursory phases or protracted steady volcanism over longer (several Myr) timescales.

As geochronologic precision surpasses  $\pm 0.05\%$ , variations in time-averaged volcanic output within the main phase have emerged, although hiatus durations are controversial<sup>139, 142, 143, 145</sup>. Variations in the intensity of volcanic activity also find support from paleomagnetic records<sup>146-148</sup> and coeval records of sedimentary Hg<sup>5, 149-151</sup>, which leverage the role of volcanoes as a dominant source of environmental Hg to reconstruct province-scale activity intensity from sedimentary records. Beyond the debate regarding the tempo of eruptive activity, a further key question is whether the main phase of volcanism is, or is not, the primary driver of the environmental crises associated with many LIPs (Box 1), as it is the pace of volatile release rather than lava flux that is the main determinant of global environmental changes.

Most continental LIPs also host more minor formations that predate and postdate the main phase. These formations, often alkaline in composition and less well preserved for older LIPs, record magmatism over a time period up to ~10 Myr or occasionally even longer<sup>152</sup>. LIP eruption fluxes seem to vary by more than an order of magnitude across formations<sup>143</sup>. It is an open question how such variations relate to transitions in the magnitude of excess mantle melting<sup>153</sup>, to the

effective crustal hydraulic connection between mantle source and the surface<sup>81</sup>, or perhaps in some cases to external perturbations (such as the Chicxulub meteor impact in the case of Deccan Traps<sup>67</sup>).

In contrast with the more consistent <1 Myr duration of the main phase of continental LIPs, geochronology at oceanic LIPs revealed protracted high-flux magmatism spanning ~30 Myr at the Kerguelen plateau<sup>154</sup>, similar to the duration of OJP magmatism<sup>155</sup>. Indeed, the Kerguelen plateau has been linked to the 132 Ma Comei-Bunbury LIP<sup>2, 156</sup>, potentially extending the overall lifespan of the LIP to ~40 Myr. This divergence between the lifespan of continental and oceanic LIPs suggests that the lithosphere, and its influence on mantle melting, plays a strong role in modulating the tempo of surface volcanism.

## ***[H2] Tempo at the member and individual eruption scale***

Magmatic tempo on timescales of  $10^3$ - $10^4$  years is likely mediated by magma chamber dynamics<sup>81, 82</sup>, which represent a nonlinear transfer function between slowly varying melt flux from the mantle and episodic surface eruptions. Melt aggregation also homogenizes magma compositions through cycles of recharge, eruption, and fractional crystallization<sup>46, 157, 158</sup>.

These transcrustal-scale magma dynamics control the environmental impacts of LIPs. For volcanic sulfate aerosols and halogens, which have lifetimes on the order of months to years in the stratosphere (much shorter than the full duration of main phase magmatism), the duration and magnitude of emissions during individual eruptive events critically controls global climate impacts<sup>16, 159, 160</sup>. Constraining the tempo of LIP volcanism and degassing at the decadal to centennial scale is thus critical, but this temporal resolution remains beyond the limit of geochronology.

Evidence from lava flow morphology, paleomagnetic measurements and chemical box modeling suggest emplacement rates of  $100\text{s km}^3 \text{ yr}^{-1}$  (Figure 4) lasting on the order of decades to centuries<sup>146, 147, 161, 162</sup>. Additional constraints on the longevity of active eruption can be extracted from near-surface geothermometry of host rocks in the vicinity of feeder dikes, which record the time-evolving passage of magma. The Maxwell Lake feeder dike of the ~40,000  $\text{km}^3$  Wapshilla member of the CRB, representing multiple individual eruptions<sup>135</sup>, has been constrained by petrography associated with partial melt of granitoid host rocks, resetting of paleomagnetic directions, low-temperature (U-Th)/He thermochronology, oxygen isotopes and thermal modeling, to have sustained magma flow for 1-6 years<sup>163, 164</sup>. Given the known geometry and likely range of total erupted volume, this implies eruption rates of  $1\text{-}8 \text{ km}^3 \text{ day}^{-1}$  for individual eruptions of the Wapshilla member associated with this dike<sup>164</sup>.

Sedimentary layers interbedded with volcanic rocks provide a complementary view of eruptive tempo. Weathering boles intercalated with lavas in the Deccan Traps have been interpreted as a record of hiatuses in volcanic activity<sup>165</sup>. In the CAMP in Eastern North America, well-developed sedimentary sequences several hundred meters thick are interbedded with unusually thick (reaching >100 m) lava flows<sup>166, 167</sup>. In contrast, the main Siberian Traps volcanic sequences do not contain thick paleosols or sedimentary layers<sup>168</sup>. The causes of these apparent differences in eruptive tempo amongst LIPs are not known.

Taken together, existing geochronology, thermochronology, paleomagnetism, modeling, and field evidence suggest that volcanic fluxes during the most intense episodes of volcanism can be orders of magnitude higher than the longer-term average volcanic fluxes constrained by geochronology (Figure 4). This behavior, on a smaller scale, is also observed in active settings such as Iceland and Hawaii, which supports the notion that processes modulating magma tempo during LIPs sit on a continuum of magmatic activity seen elsewhere.

## ***[H2] Petrologic evolution encoded in eruptive stratigraphies***

Exposures of km-thick LIP volcanic sequences comprising hundreds of stacked lavas, along with drill cores, provide a unique record of geochemical evolution within and amongst LIPs. Geochemical progressions reflect the combined influences of mantle melt sources, fractionation, crustal contamination, and post-emplacement alteration<sup>169</sup>. Variation in isotope, major, and trace element compositions can be used to parse these processes<sup>157</sup>. Sr, Nd, Pb, and Os isotope systems are long-standing tools to trace mantle lithospheric and crustal contamination; Re-Os can also be used to resolve the timing of volcanism through seawater chemistry<sup>53, 170-172</sup>.

Member-level geochemistry from the CRB (Figure 3) shows a progression from primitive, high-MgO lavas to homogeneous, lower-MgO Grande Ronde lavas, to the heterogeneous chemistry of late-phase Saddle Mountain Basalts. This late geochemical variability is also seen in the Deccan Traps in the form of alkaline eruptions millions of years after a much more homogeneous main phase<sup>173</sup> and, along with smaller eruption volumes, indicates that LIPs undergo a protracted waning phase.

Crystal chemical and textural records from LIPs hold vast unexploited potential. For example, many lavas contain crystal aggregates known as glomerocrysts<sup>61, 174</sup>, which in other settings have been interpreted as potential records of conditions in mushy reservoirs<sup>175</sup>. Other flood basalt lavas are strikingly phenocryst poor<sup>176, 177</sup>. Interrogation of crystal-scale diffusion records

<sup>178, 179</sup> could dramatically improve constraints on ascent timescales and storage conditions of LIP  
magmas.

## **[H2] Eruptive style**

The frequency of large silicic eruptions associated with dominantly basaltic LIPs remains  
an open question (see <sup>122, 180</sup> for reviews of dominantly silicic LIPs). However, silicic volcanism  
is a common observation. For example, the Parana-Etendeka, CRB, and Deccan provinces <sup>181-183</sup>  
all host subordinate silicic volcanism, as well the oceanic Kerguelen Plateau LIP, which culminated  
with episodes of explosive felsic volcanism <sup>64</sup>. Silicic eruptions have been linked to dispersal of Pb  
<sup>184</sup> and produce copious ash that has been hypothesized to drive ocean fertilization <sup>185</sup>.

Nonetheless, LIPs are generally dominated by basaltic styles of eruption. As the explosive  
products of LIP volcanism are rarely preserved, interpretation of the style of LIP volcanism is often  
grounded in historical observations. The degree of explosivity of these events is an important  
question because sulfur and halogen injection altitude strongly control their lifetime in the  
atmosphere <sup>159, 186</sup> and the eruption column and gas plume heights depend on eruptive style and  
intensity <sup>187</sup>.

Based on detailed physical volcanology and first-hand accounts <sup>188, 189</sup>, the 1783-1784 Laki  
eruption in Iceland might be considered the ‘type-example’ LIP analog: a sequence of 14 episodes  
over a 27 km en echelon set of dike segments, each episode characterized by a rapid waxing and  
longer waning of effusive flux, with violent fire-fountaining and Strombolian behavior at the vent  
that produced minor tephra along with prodigious amounts of lava totaling  $14.7 \pm 1$  km<sup>3</sup> over 8  
months (Figure 4). Vent-proximal explosive deposits, lava flow morphology (specifically inflation  
features that promote long-distance transport <sup>190</sup>), and evidence for time-progressive localization of  
the feeder dike surface vent locations, are all documented in LIPs <sup>191, 192</sup>. Scaled experiments can  
capture complex fluid behavior underlying vent evolution <sup>193</sup>, and in concert with multiphase  
modeling of bubbles and crystals in low-viscosity magmas <sup>194, 195</sup>, they offer a path to understanding  
the shallow magma dynamics that influence degassing and eruptive style.

Tephra deposits associated with the Roza unit of the CRB have been linked to fire fountains  
reaching >1000 m in height <sup>192</sup>. For comparison, Laki fire fountains reached an estimated 800-1450  
m <sup>196</sup>, and fire fountains from the Holuhraun 2014-2015 fissure eruption in Iceland reached  
approximately ~126 m <sup>197</sup>. Magma-water interactions can also produce explosive activity and  
voluminous proximal volcanoclastic rocks <sup>198</sup>. However, to date few substantial airfall ash deposits  
have been linked with flood basalt activity, reflecting the weak preservation potential of such  
lithologies, the ash-poor character of fire-fountaining, and relatively low eruption column heights.

Notable gas plumes can also loft above fissure-fed fire fountains. Laki fire-fountains were estimated to have sustained eruption columns of up to 15-km altitude<sup>172</sup>, based on historical reports from contemporary observers, facilitating sulfur injection to the upper troposphere and lower stratosphere. In oceanic plateaus, high water:magma ratios favor a combination of submarine lavas, hyaloclastites, and intervals of subaerial volcanism accompanied by phreatomagmatic explosive activity<sup>199</sup>.

## **[H1] Redistribution of volatiles**

Volatile release during LIP activity represents one of the primary links between magmatism and global environmental changes. Volatiles are also among the main drivers of eruptions. The sources, transfer, and release of volatiles, and the petrologic controls that modulate fluxes to the atmosphere, are discussed here.

## **[H2] Volatile sources and budgets**

LIP volatiles originate from the deep mantle, the CLM, and the crust (through assimilation and metamorphism). Volatiles such as water, CO<sub>2</sub> and the halogens (with the exception of F<sup>200</sup>) are often strongly incompatible [G] during mantle melting, corresponding to bulk distribution coefficients [G] << 1. Therefore, the total mass of these volatiles extracted from a parcel of mantle undergoing melting does not change appreciably for melt fractions above a few percent. Instead, increasing melt fraction just generates larger volumes of melt, diluting volatile concentrations in the resulting magma.

Consequently, it is the volume of mantle that undergoes melting and the initial volatile contents of the mantle source—rather than the volume of melt generated or the melt fraction—that primarily dictates the overall magnitude of volatile mobilization from the deep mantle. Mantle volatile concentrations could be heterogeneous during LIP melting. For example, estimated carbon concentrations in the deep and upper mantle are 50-500 ppm C and 10-30 ppm C, respectively<sup>201</sup>, and mantle carbon and halogen enrichments due to recycled oceanic crust in the plume source have been suggested for the Siberian Traps<sup>34</sup>.

In contrast with the incompatibility of CO<sub>2</sub>, H<sub>2</sub>O, and Cl, the behavior of S during mantle melting is more complex. Evidence from mantle xenoliths and diamond inclusions suggests that sulfides are common in the mantle; these sulfides likely control S concentrations in the melt until they are exhausted from the mantle source (~16% of aggregate fractional melting, assuming 140



ppm S in the mantle source)<sup>202</sup>. Main phase tholeiitic magmas in which melt fractions can exceed 30% might no longer be in equilibrium with mantle sulfide; fluctuations in sulfur saturation state shallower in the magmatic plumbing system can further complicate the magmatic sulfur budget<sup>202</sup>.

Ancient CLM is emerging as a major—but poorly quantified—reservoir of volatiles, including halogens, sulfur, and both reduced and oxidized carbon, that accumulate on very long timescales due to percolation and freezing of melts and fluids from the underlying mantle<sup>10, 50, 203-205</sup>. LIP magmatism and rifting—sometimes operating in tandem—appear to be among the few geologic processes capable of disrupting and rejuvenating the long-lived CLM reservoir<sup>206</sup>. CLM contributions to LIP magma volatile contents could be substantial but are poorly constrained. Xenolith studies focusing on samples from kimberlites that predate and postdate LIP emplacement<sup>204, 207</sup>, as well as kimberlites directly associated with LIPs<sup>208</sup>, offer promising means to gain snapshots of both the volatile budget of the CLM, and the extent to which LIP activity can mobilize these volatiles. Percolation of low-degree melts on the margins of mantle plumes can also be a mechanism for replenishing CLM volatiles<sup>10</sup>. As oceanic plates lack >180 Ma lithospheric mantle, the lack of volatile release from the CLM may contribute to more muted climate consequences of oceanic plateaus relative to continental LIPs<sup>203</sup>.

The crustal rocks into which LIP magmas intrude provide another potential explanation for differences in volatile release between LIPs. The degree of environmental stress caused by continental LIP volcanism has been correlated with the types of country rock intruded<sup>189</sup>. Crustal rocks such as carbonates, shales, hydrocarbon-bearing source rocks, evaporites, and coals can release volatiles (for example, CO<sub>2</sub>, hydrocarbons, halocarbons and Hg) to the environment via melting and assimilation into the magma or thermal metamorphism and direct release (Box 1). By some estimates, carbon release owing to metamorphism can be an order of magnitude larger than that from mantle melting<sup>209, 210</sup>, though both mantle and crustal carbon release are poorly constrained and quantifying these fluxes for carbon, as well as for other volatiles, is a major focus of current research<sup>11, 91, 211, 212</sup>. Other factors could also be important. For example, in addition to the absence of ancient CLM and fewer volatile-rich host rocks during emplacement of oceanic LIPs, degassing and atmospheric injection of sulfur, halogens and other volatiles are likely impeded during submarine eruptions.

## **[H2] Magnitude of volatile release**

Determining the comparative release of volatiles from the deep mantle, the CLM, and the crust—although critical to assessing why and how LIPs trigger surface environmental changes—is



challenging (see Box 1 for data from the Siberian Traps highlighting existing constraints from each of these sources and remaining gaps). Furthermore, due to changes in melting conditions and transport through the crust, volatile release is probably not evenly distributed through the span of LIP emplacement. Rather, release of CO<sub>2</sub>, halogens, and sulfur might each evolve semi-independently through the course of LIP magmatism.

Melt inclusions—tiny ‘time capsules’ of melt trapped inside crystals that can record pre-eruptive volatiles—provide snapshots of volatiles in LIP magmas (Figure 5), subject to corrections for post-entrapment processes such as diffusion, shrinkage bubble formation, and crystallization. Within melt inclusions, CO<sub>2</sub> often partitions into vapor bubbles (Figure 1h) that likely commonly contain the majority of CO<sub>2</sub> <sup>212-214</sup>. Along with **rehomogenization [G]**, Raman spectroscopy is emerging as an important technique to account for CO<sub>2</sub> in such bubbles to more accurately reconstruct CO<sub>2</sub> in ascending LIP magmas <sup>211, 212</sup>. Even when corrected for post-entrapment processes, melt inclusions often trap already partially degassed melts—in particular with respect to CO<sub>2</sub>, which can saturate deep in the magmatic system (Figures 2, 5). Therefore, non-volatile trace elements that behave similarly to volatiles during melting can provide proxies for the initial, pre-degassing melt concentrations (for example, Ba for CO<sub>2</sub> and Nd for F) <sup>11, 212, 213, 215, 216</sup>. Halogen data (Figure 5, panels c-f) suggest oceanic LIPs could serve as a useful testing ground for this approach. Fluorine and Nd data from OJP <sup>65</sup> plot close to F/Nd=21 <sup>216</sup>, whereas CRB F/Nd ratios <sup>217</sup> are more scattered, suggesting that oceanic plateaus can record mantle melting more cleanly.

Melt inclusions and other proxies can give insights into the variability of degassing between the different phases of LIPs. The Siberian Traps show evidence for relatively high CO<sub>2</sub> and halogens in melt inclusions from early and late alkaline magmas (Figure 5), thought to originate from deep, low-degree melting <sup>58, 61, 172, 218</sup> (see also Figure 2). The extent to which other LIPs host similarly volatile-rich magmas is uncertain, largely due to generally sparse melt inclusion data for alkaline magmas. In general, CO<sub>2</sub> and halogens show substantial variability from LIP to LIP (Figure 5). Sulfur concentrations are fairly consistent across LIPs, between phases and with proxy constraints (for example, FeO<sub>Total</sub> Ref. <sup>219</sup>), despite changes in melting conditions, suggesting buffering of sulfur concentrations during magma ascent <sup>202</sup>.

Volatiles can be dissolved in, and thus move with, magma. However, there are multiple modes of volatile transport that effectively decouple volatile from magmatic fluxes. CO<sub>2</sub> is expected to dominate the exsolved phase with increasing depth owing to the strong pressure-dependence of CO<sub>2</sub> solubility in silicate melts (Figure 1). Ascent of this CO<sub>2</sub>-rich exsolved phase, known as **CO<sub>2</sub> flushing [G]**, adds to the volatile mass of shallower melts <sup>220</sup>. Even stronger decoupling between volcanism and outgassing is possible in the case of fluids or vapors—either

exsolved from magmas or released via metamorphism of country rocks—that escape through high-permeability regions in the crust<sup>93, 209, 221</sup>.

Very high non-eruptive CO<sub>2</sub> fluxes from modern basaltic systems<sup>222, 223</sup> attest to the potential importance of diffuse degassing (also known as cryptic degassing). Quantifying the relative importance of cryptic degassing—especially for intrusive LIP magmas, which could represent the majority of magma volume, and especially in relation to the overall evolution of the magmatic system—is a major unresolved challenge. Driven by changes in mantle-derived volatiles and ascent of exsolved gases, the tempo of volatile release can decouple strongly from the tempo of volcanic eruptions at the surface<sup>11</sup>. This decoupling might explain apparent temporal offsets between peak volcanic fluxes and episodes of global warming during CRB and Deccan magmatism<sup>138, 212, 224</sup>.

Sulfur exsolution into H<sub>2</sub>O-CO<sub>2</sub> dominated bubbles can be complex. **Magma redox [G]**, which is poorly constrained for LIPs, controls sulfur speciation and volatility<sup>225</sup>, and influences saturation of a sulfide phase that buffers melt S concentrations<sup>226</sup>. Immiscible sulfide globules can scavenge metals and chalcophile elements<sup>227, 228</sup>. Unlike dissolved volatiles, both bubbles and sulfide liquids can be mobile with respect to the melt, thereby decoupling from volcanic output rates. While sulfides are dense and would re-sequester their volatiles upon sinking, attachment to bubbles has been proposed as a mechanism to buoy metal-bearing sulfides to reach the atmosphere under some circumstances<sup>228</sup>. In addition to sulfur flux, the climate response to sulfur outgassing also depends on emission duration, altitude, latitude, and background climate<sup>159, 229</sup>.

## **[H1] The evolution of LIP magmatic systems**

LIP magmatic systems represent large-scale end-members for volcanic activity on Earth and other planets. Variable magma supply and crustal rheology help define regimes of magma transport and storage<sup>81</sup> (Figure 6) that offer generalizable insights into how volcanism works on large spatial and temporal scales. We suggest a conceptual model for the life cycle of continental LIPs to parallel thermomechanical changes hypothesized for other types of volcanic systems<sup>230</sup>. Initial mantle melts encounter a thermally immature crust, promoting rapid heating associated with freezing of smaller reservoirs. As the crust warms, ductile deformation increasingly dominates the crust's mechanical response to magma-induced stresses. Magma buoyancy, competing with time-evolving recharge from the mantle, results in hydraulic integration of storage zones, dike propagation, and ultimately magma ascent<sup>81, 82</sup> establishing a robust transcrustal magma transport network during the main phase.

The onset, main phase, and decline of the CRB is relatively well-established. However, the extent to which other LIPs follow this progression remains unclear, in part because high-precision geochronology tracking oceanic, alkaline, and intrusive magmas is sparse. High-precision geochronologic data spanning the full duration of oceanic and continental LIPs—in particular for alkaline, ultramafic, and intrusive rocks—are needed to assess when LIPs follow, and when they depart from, the trajectory illustrated in Figure 6. We expect the life cycle of oceanic LIPs to reflect a lower degree of thermal maturation of crustal host rocks due to efficient hydrothermal cooling of the thinner oceanic crust. Whether the progression of LIP eruptions can be linked to cyclic destabilization of individual <sup>230</sup> or perhaps many linked <sup>231</sup> magma chambers represents a key question required to further integrate LIPs into the spectrum of magmatism.

While intense debate has surrounded the origins of large-scale melting, less work has focused on the death of LIPs. Yet, both waning magma supply and ductile crust—capable of accommodating new magma as intrusions—could reduce surface volcanism. This transition to a storage-dominated regime raises the possibility that emplacement and differentiation of Moho-depth intrusions could continue long after the cessation of most extrusive volcanic activity.

## **[H1] Summary and future perspectives**

LIPs have a life cycle. Melting initiates, the first lavas erupt, large volumes of magma are emplaced rapidly ( $10^4$ - $10^6$  yrs for continental LIPs) in the lithosphere and at the surface with a tempo that varies from province to province. LIPs end over a longer waning phase ( $10^6$ - $10^7$  yrs for continental LIPs) with heterogeneous surface eruptions. Through this life cycle, LIPs mobilize volatiles from the deep mantle, mantle lithosphere, and crust, underpinning proposed links with some of the most abrupt changes in surface environments in the past half-billion years of Earth's history.

The majority of continental LIP magmas likely do not erupt, but the nature and consequences of intrusive magmas are more poorly known than their erupted counterparts. Improved geophysical and petrologic constraints on intrusive LIP magmas are critically needed to understand their evolution, environmental repercussions, and role in economic ore formation. In particular, there are opportunities to reconcile geodynamic modelling of melt generation and seismic imaging of the deeper crustal transport system with other constraints on the LIP life cycle.

Fluxes of LIP lava erupted at the surface are also highly variable and need further constraints, as estimates of maximum eruption rates during LIP activity span two orders of magnitude. The highest estimates imply volcanic fluxes of  $10^2$ - $10^3$  km<sup>3</sup> year<sup>-1</sup> (Refs. <sup>147, 164, 232</sup>),

631 suggesting that the majority of lava volume from some LIPs could have erupted over durations of  
632  $<10^4$  years. New techniques—for example from paleomagnetism or thermochronology—are  
633 needed to constrain durations and intensities of eruptive episodes and hiatuses.

634 LIP activity and continental rifting are among the few processes capable of dismembering  
635 and rejuvenating ancient continental lithospheric mantle. Therefore, they potentially play a unique  
636 role in solid Earth volatile cycling. Studies of alkaline magmas and mantle xenoliths—either  
637 directly associated with LIPs, or erupted to the surface before or after LIP emplacement—offer  
638 complementary perspectives on the evolution of the mantle lithosphere and interactions with LIPs.

639 The redox state of the CLM is thought to be highly heterogeneous, and therefore data  
640 constraining the redox evolution of tholeiitic and alkaline LIP magmas could provide a unique  
641 window into mantle processes<sup>50, 205, 233</sup>. Volatiles such as CO<sub>2</sub>, S, Cl, and F are relatively easily  
642 measured through traditional analytical techniques, but existing datasets reveal broad diversity in  
643 volatile budgets of LIP magmas, motivating further efforts to constrain volatiles, particularly for  
644 oceanic plateaus and different stages of LIP activity. Developing new analytical techniques and  
645 datasets to track the behavior and fluxes of lower-concentration (but environmentally impactful)  
646 Hg, Br, and trace metals are also needed to understand their degassing behavior and imprint in  
647 sedimentary records<sup>162, 184, 227</sup>.

648 Evolving volatile concentrations and the mobility of exsolved and metamorphic gases can  
649 cause the tempo of gas release to diverge from the extrusive flux. Tracking the transfer of volatiles  
650 within the magmatic system and through the crust, and exploring how the resulting volatile fluxes  
651 evolve through the life cycle of LIPs, provides a critical link between mantle melting and  
652 environmental perturbations. We urge adaptation of techniques from studies of volatiles in other  
653 volcanic settings (ranging from scaled experiments to multi-phase modelling to trace element  
654 proxies for mantle volatiles) to investigate complex LIP systems.

655 Ultimately, we see a need to align increasingly high-resolution geochronologically- and  
656 astrochronologically-paced paleoclimate records with similarly resolved timelines of magmatic  
657 processes to understand how LIPs can plausibly cause such profound changes in climate and why  
658 those shifts occur when they do. A central issue threading through these challenges is varying  
659 timescales: the processes that link melt generation in the mantle to surface outgassing have  
660 characteristic durations from seconds to millions of years. Understanding the multiple timescales  
661 that characterize LIP magmatic processes is an essential step towards reconciling large-scale  
662 volcanism with deep mantle drivers and disruption and change in Earth's surface climate.

## References

1. Bryan, S. E. & Ernst, R. E. Revised definition of large igneous provinces (LIPs). *Earth-Sci. Rev.* **86**, 175-202 (2008).
2. Ernst, R. E. *et al.* Large Igneous Province Record Through Time and Implications for Secular Environmental Changes and Geological Time-Scale Boundaries. *Large Igneous Provinces: A Driver of Global Environmental and Biotic Changes*, 1-26 (2020).
3. Coffin, M. F. & Eldholm, O. Large igneous provinces: crustal structure, dimensions, and external consequences. *Rev. Geophys.* **32**, 1-36 (1994).
4. Ernst, R. E. in *Large igneous provinces* (Cambridge University Press, 2014).
5. Jones, M. T., Jerram, D. A., Svensen, H. H. & Grove, C. The effects of large igneous provinces on the global carbon and sulphur cycles. *Palaeogeogr. , Palaeoclimatol. , Palaeoecol.* **441**, 4-21 (2016).
6. Bond, D. P. & Wignall, P. B. Large igneous provinces and mass extinctions: an update. *Volcanism, Impacts, and Mass Extinctions: Causes and Effects* **505**, 29-55 (2014).
7. Wignall, P. Large igneous provinces and mass extinctions. *Earth-Sci. Rev.* **53**, 1-33 (2001).
8. Courtillot, V., Davaille, A., Besse, J. & Stock, J. Three distinct types of hotspots in the Earth's mantle. *Earth Planet. Sci. Lett.* **205**, 295-308 (2003).
9. Clapham, M. E. & Renne, P. R. Flood basalts and mass extinctions. *Annu. Rev. Earth Planet. Sci.* **47**, 275-303 (2019).
10. Foley, S. F. & Fischer, T. P. An essential role for continental rifts and lithosphere in the deep carbon cycle. *Nature Geoscience* **10**, 897 (2017).
11. Black, B. A. & Gibson, S. A. Deep carbon and the life cycle of large igneous provinces. *Elements: An International Magazine of Mineralogy, Geochemistry, and Petrology* **15**, 319-324 (2019).
12. Ernst, R. E., Liikane, D. A., Jowitt, S. M., Buchan, K. & Blanchard, J. A new plumbing system framework for mantle plume-related continental Large Igneous Provinces and their mafic-ultramafic intrusions. *J. Volcanol. Geotherm. Res.* **384**, 75-84 (2019).
13. Ernst, R., Grosfils, E. & Mege, D. Giant dike swarms: Earth, venus, and mars. *Annu. Rev. Earth Planet. Sci.* **29**, 489-534 (2001).
14. Buchan, K. L. & Ernst, R. E. Plumbing systems of large igneous provinces (LIPs) on Earth and Venus: Investigating the role of giant circumferential and radiating dyke swarms, coronae and novae, and mid-crustal intrusive complexes. *Gondwana Research* (2021).

15. Ernst, R. E. & Youbi, N. How Large Igneous Provinces affect global climate, sometimes cause mass extinctions, and represent natural markers in the geological record. *Palaeogeogr. , Palaeoclimatol. , Palaeoecol.* **478**, 30-52 (2017).
16. Self, S., Schmidt, A. & Mather, T. Emplacement characteristics, time scales, and volcanic gas release rates of continental flood basalt eruptions on Earth. *Geological Society of America Special Papers* **505**, SPE505-16 (2014).
17. Campbell, I. H. Testing the plume theory. *Chem. Geol.* **241**, 153-176 (2007).
18. Foulger, G. R. in *Plates vs Plumes: A Geological Controversy* (Wiley-Blackwell, 2011).
19. Richards, M. A., Duncan, R. A. & Courtillot, V. E. Flood basalts and hot-spot tracks: plume heads and tails. *Science* **246**, 103-107 (1989).
20. Campbell, I. H. & Griffiths, R. W. Implications of mantle plume structure for the evolution of flood basalts. *Earth Planet. Sci. Lett.* **99**, 79-93 (1990).
21. Elkins-Tanton, L. T. & Hager, B. H. Melt intrusion as a trigger for lithospheric foundering and the eruption of the Siberian flood basalts. *Geophysical Research Letters* **27**, 3937-3940 (2000).
22. Jones, A. P., Price, G. D., Price, N. J., DeCarli, P. S. & Clegg, R. A. Impact induced melting and the development of large igneous provinces. *Earth Planet. Sci. Lett.* **202**, 551-561 (2002).
23. Coltice, N., Phillips, B., Bertrand, H., Ricard, Y. & Rey, P. Global warming of the mantle at the origin of flood basalts over supercontinents. *Geology* **35**, 391-394 (2007).
24. Gurnis, M. Large-scale mantle convection and the aggregation and dispersal of supercontinents. *Nature* **332**, 695-699 (1988).
25. French, S. W. & Romanowicz, B. Broad plumes rooted at the base of the Earth's mantle beneath major hotspots. *Nature* **525**, 95-99 (2015).
26. Stuart, F. M., Lass-Evans, S., Fitton, J. G. & Ellam, R. M. High  $^3\text{He}/^4\text{He}$  ratios in picritic basalts from Baffin Island and the role of a mixed reservoir in mantle plumes. *Nature* **424**, 57-59 (2003).
27. Peters, B. J. *et al.* Helium--oxygen--osmium isotopic and elemental constraints on the mantle sources of the Deccan Traps. *Earth Planet. Sci. Lett.* **478**, 245-257 (2017).
28. Thompson, R. & Gibson, S. Transient high temperatures in mantle plume heads inferred from magnesian olivines in Phanerozoic picrites. *Nature* **407**, 502-506 (2000).
29. Herzberg, C. & Gazel, E. Petrological evidence for secular cooling in mantle plumes. *Nature* **458**, 619-622 (2009).

- 729 30. Coogan, L., Saunders, A. & Wilson, R. Aluminum-in-olivine thermometry of primitive  
730 basalts: Evidence of an anomalously hot mantle source for large igneous provinces. *Chem. Geol.*  
731 **368**, 1-10 (2014).
- 732 31. Davies, D., Goes, S. & Sambridge, M. On the relationship between volcanic hotspot  
733 locations, the reconstructed eruption sites of large igneous provinces and deep mantle seismic  
734 structure. *Earth Planet. Sci. Lett.* **411**, 121-130 (2015).
- 735 32. Garnero, E. J., McNamara, A. K. & Shim, S. Continent-sized anomalous zones with low  
736 seismic velocity at the base of Earth's mantle. *Nature Geoscience* **9**, 481-489 (2016).
- 737 33. Koppers, A. A. *et al.* Mantle plumes and their role in Earth processes. *Nature Reviews Earth*  
738 *& Environment*, 1-20 (2021).
- 739 34. Sobolev, S. V. *et al.* Linking mantle plumes, large igneous provinces and environmental  
740 catastrophes. *Nature* **477**, 312-U80 (2011).
- 741 35. Herzberg, C. *et al.* Nickel and helium evidence for melt above the core–mantle boundary.  
742 *Nature* **493**, 393-397 (2013).
- 743 36. Trela, J. *et al.* The hottest lavas of the Phanerozoic and the survival of deep Archaean  
744 reservoirs. *Nature Geoscience* **10**, 451-456 (2017).
- 745 37. Farnetani, C. G. & Richards, M. A. Numerical investigations of the mantle plume initiation  
746 model for flood basalt events. *Journal of Geophysical Research: Solid Earth* **99**, 13813-13833  
747 (1994).
- 748 38. Jennings, E. S., Gibson, S. A. & MacLennan, J. Hot primary melts and mantle source for the  
749 Paran\`a-Etendeka flood basalt province: New constraints from Al-in-olivine thermometry. *Chem.*  
750 *Geol.* **529**, 119287 (2019).
- 751 39. Spice, H. E., Fitton, J. G. & Kirstein, L. A. Temperature fluctuation of the Iceland mantle  
752 plume through time. *Geochem. Geophys. Geosyst.* **17**, 243-254 (2016).
- 753 40. Kamenetsky, V. S., Chung, S., Kamenetsky, M. B. & Kuzmin, D. V. Picrites from the  
754 Emeishan Large Igneous Province, SW China: a compositional continuum in primitive magmas  
755 and their respective mantle sources. *J. Petrol.* **53**, 2095-2113 (2012).
- 756 41. Lightfoot, P. C. *et al.* Remobilization of the continental lithosphere by a mantle plume:  
757 Major-, trace-element, and Sr-, Nd- and Pb-isotopic evidence from picritic and tholeiitic lavas of  
758 the Noril'sk district, Siberia. *Contributions to Mineralogy and Petrology* **114**, 171-188 (1993).
- 759 42. Camp, V. E. & Hanan, B. B. A plume-triggered delamination origin for the Columbia River  
760 Basalt Group. *Geosphere* **4**, 480-495 (2008).
- 761 43. Pearce, J. A., Ernst, R. E., Peate, D. W. & Rogers, C. LIP printing: Use of immobile element  
762 proxies to characterize Large Igneous Provinces in the geologic record. *Lithos*, 106068 (2021).



- 763 44. Shorttle, O. & MacLennan, J. Compositional trends of Icelandic basalts: Implications for  
764 short-length scale lithological heterogeneity in mantle plumes. *Geochem. Geophys. Geosyst.* **12**  
765 (2011).
- 766 45. Kent, A. *et al.* Mantle heterogeneity during the formation of the North Atlantic igneous  
767 province: Constraints from trace element and Sr-Nd-Os-O isotope systematics of Baffin Island  
768 picrites. *Geochem. Geophys. Geosyst.* **5** (2004).
- 769 46. Cox, K. A model for flood basalt vulcanism. *J. Petrol.* **21**, 629-650 (1980).
- 770 47. Alt, J. C. *et al.* Recycling of water, carbon, and sulfur during subduction of serpentinites: A  
771 stable isotope study of Cerro del Almirez, Spain. *Earth Planet. Sci. Lett.* **327**, 50-60 (2012).
- 772 48. Hofmann, A. W. & White, W. M. Mantle plumes from ancient oceanic crust. *Earth Planet.*  
773 *Sci. Lett.* **57**, 421-436 (1982).
- 774 49. Sobolev, A. V. *et al.* The amount of recycled crust in sources of mantle-derived melts.  
775 *Science* **316**, 412-417 (2007).
- 776 50. Stagno, V., Ojwang, D. O., McCammon, C. A. & Frost, D. J. The oxidation state of the  
777 mantle and the extraction of carbon from Earth's interior. *Nature* **493**, 84-88 (2013).
- 778 51. Cabral, R. A. *et al.* Anomalous sulphur isotopes in plume lavas reveal deep mantle storage of  
779 Archaean crust. *Nature* **496**, 490-493 (2013).
- 780 52. Wang, X. J. *et al.* Recycled ancient ghost carbonate in the Pitcairn mantle plume. *Proc. Natl.*  
781 *Acad. Sci. U. S. A.* **115**, 8682-8687 (2018).
- 782 53. Wooden, J. L. *et al.* Isotopic and trace-element constraints on mantle and crustal contributions  
783 to Siberian continental flood basalts, Noril'sk area, Siberia. *Geochim. Cosmochim. Acta* **57**, 3677-  
784 3704 (1993).
- 785 54. Gibson, S., Thompson, R. & Day, J. Timescales and mechanisms of plume-lithosphere  
786 interactions: <sup>40</sup>Ar/<sup>39</sup>Ar geochronology and geochemistry of alkaline igneous rocks from the  
787 Paraná-Etendeka large igneous province. *Earth Planet. Sci. Lett.* **251**, 1-17 (2006).
- 788 55. Herzberg, C. & O'hara, M. Plume-associated ultramafic magmas of Phanerozoic age. *J.*  
789 *Petrol.* **43**, 1857-1883 (2002).
- 790 56. White, R. & McKenzie, D. Mantle plumes and flood basalts. *Journal of Geophysical*  
791 *Research: Solid Earth* **100**, 17543-17585 (1995).
- 792 57. Lee, C. A., Luffi, P., Plank, T., Dalton, H. & Leeman, W. P. Constraints on the depths and  
793 temperatures of basaltic magma generation on Earth and other terrestrial planets using new  
794 thermobarometers for mafic magmas. *Earth Planet. Sci. Lett.* **279**, 20-33 (2009).
- 795 58. Sobolev, A. V., Sobolev, S. V., Kuzmin, D., Malitch, K. & Petrunin, A. Siberian  
796 meimechites: origin and relation to flood basalts and kimberlites. *Russ. Geol. Geophys.* **50**, 999-  
797 1033 (2009).



- 798 59. Herzberg, C. Partial melting below the Ontong Java Plateau. *Geological Society, London,*  
799 *Special Publications* **229**, 179-183 (2004).
- 800 60. White, R. & McKenzie, D. Magmatism at rift zones: the generation of volcanic continental  
801 margins and flood basalts. *Journal of Geophysical Research: Solid Earth* **94**, 7685-7729 (1989).
- 802 61. Fedorenko, V., Czamanske, G., Zen'ko, T., Budahn, J. & Siems, D. Field and geochemical  
803 studies of the melilite-bearing Arydzhangsky Suite, and an overall perspective on the Siberian  
804 alkaline-ultramafic flood-volcanic rocks. *International Geology Review* **42**, 769-804 (2000).
- 805 62. Simonetti, A. & Neal, C. R. In-situ chemical, U--Pb dating, and Hf isotope investigation of  
806 megacrystic zircons, Malaita (Solomon Islands): Evidence for multi-stage alkaline magmatic  
807 activity beneath the Ontong Java Plateau. *Earth Planet. Sci. Lett.* **295**, 251-261 (2010).
- 808 63. Frey, F. A. *et al.* Temporal geochemical trends in Kerguelen Archipelago basalts: evidence  
809 for decreasing magma supply from the Kerguelen plume. *Chem. Geol.* **164**, 61-80 (2000).
- 810 64. Frey, F. A. *et al.* Origin and evolution of a submarine large igneous province: the Kerguelen  
811 Plateau and Broken Ridge, southern Indian Ocean. *Earth Planet. Sci. Lett.* **176**, 73-89 (2000).
- 812 65. Jackson, M. G. *et al.* Ultra-depleted melts in olivine-hosted melt inclusions from the Ontong  
813 Java Plateau. *Chem. Geol.* **414**, 124-137 (2015).
- 814 66. Weatherley, S. M. & Katz, R. F. Melting and channelized magmatic flow in chemically  
815 heterogeneous, upwelling mantle. *Geochem. Geophys. Geosyst.* **13** (2012).
- 816 67. Richards, M. A. *et al.* Triggering of the largest Deccan eruptions by the Chicxulub impact.  
817 *Geological Society of America Bulletin*, B31167. 1 (2015).
- 818 68. Thompson, R. & Gibson, S. A. Subcontinental mantle plumes, hotspots and pre-existing  
819 thinspots. *Journal of the Geological Society* **148**, 973-977 (1991).
- 820 69. Sleep, N. H. Lateral flow and ponding of starting plume material. *Journal of Geophysical*  
821 *Research: Solid Earth* **102**, 10001-10012 (1997).
- 822 70. Gao, H. Crustal seismic structure beneath the source area of the Columbia River flood basalt:  
823 Bifurcation of the Moho driven by lithosphere delamination. *Geophys. Res. Lett.* **42**, 9764-9771  
824 (2015).
- 825 71. Sharma, J., Kumar, M. R., Roy, K. S., Pal, S. & Roy, P. Low-Velocity Zones and Negative  
826 Radial Anisotropy Beneath the Plume Perturbed Northwestern Deccan Volcanic Province.  
827 *Journal of Geophysical Research: Solid Earth* **126**, e2020JB020295 (2021).
- 828 72. Niday, W. & Humphreys, E. Complex upper mantle anisotropy in the Pacific Northwest:  
829 Evidence from SKS splitting. *Earth Planet. Sci. Lett.* **540**, 116264 (2020).
- 830 73. Ridley, V. A. & Richards, M. A. Deep crustal structure beneath large igneous provinces and  
831 the petrologic evolution of flood basalts. *Geochem. Geophys. Geosyst.* **11** (2010).

- 832 74. Catchings, R. & Mooney, W. Crustal structure of the Columbia Plateau: Evidence for  
833 continental rifting. *Journal of Geophysical Research: Solid Earth* **93**, 459-474 (1988).
- 834 75. Thybo, H. & Artemieva, I. Moho and magmatic underplating in continental lithosphere.  
835 *Tectonophysics* **609**, 605-619 (2013).
- 836 76. Davenport, K., Hole, J., Tikoff, B., Russo, R. & Harder, S. A strong contrast in crustal  
837 architecture from accreted terranes to craton, constrained by controlled-source seismic data in  
838 Idaho and eastern Oregon. *Lithosphere* **9**, 325-340 (2017).
- 839 77. Oakey, G. & Saltus, R. Geophysical analysis of the Alpha–Mendeleev ridge complex:  
840 characterization of the High Arctic Large Igneous Province. *Tectonophysics* **691**, 65-84 (2016).
- 841 78. Larsen, R. B. *et al.* Portrait of a giant deep-seated magmatic conduit system: The Seiland  
842 Igneous Province. *Lithos* **296**, 600-622 (2018).
- 843 79. Grant, T. B. *et al.* Anatomy of a deep crustal volcanic conduit system; the Reinfjord  
844 ultramafic complex, Seiland Igneous Province, northern Norway. *Lithos* **252**, 200-215 (2016).
- 845 80. Lange, R. A. Constraints on the preeruptive volatile concentrations in the Columbia River  
846 flood basalts. *Geology* **30**, 179-182 (2002).
- 847 81. Karlstrom, L. & Richards, M. On the evolution of large ultramafic magma chambers and  
848 timescales for flood basalt eruptions. *Journal of Geophysical Research: Solid Earth* (1978–2012)  
849 **116** (2011).
- 850 82. Black, B. A. & Manga, M. Volatiles and the tempo of flood basalt magmatism. *Earth Planet.*  
851 *Sci. Lett.* **458**, 130-140 (2017).
- 852 83. Farnetani, C. G., Richards, M. A. & Ghiorso, M. S. Petrological models of magma evolution  
853 and deep crustal structure beneath hotspots and flood basalt provinces. *Earth Planet. Sci. Lett.*  
854 **143**, 81-94 (1996).
- 855 84. Crisp, J. A. Rates of magma emplacement and volcanic output. *J. Volcanol. Geotherm. Res.*  
856 **20**, 177-211 (1984).
- 857 85. White, S. M., Crisp, J. A. & Spera, F. J. Long-term volumetric eruption rates and magma  
858 budgets. *Geochem. Geophys. Geosyst.* **7** (2006).
- 859 86. Tierney, C. R., Schmitt, A. K., Lovera, O. M. & de Silva, S. L. Voluminous plutonism during  
860 volcanic quiescence revealed by thermochemical modeling of zircon. *Geology* **44**, 683-686  
861 (2016).
- 862 87. Ward, K. M., Delph, J. R., Zandt, G., Beck, S. L. & Ducea, M. N. Magmatic evolution of a  
863 Cordilleran flare-up and its role in the creation of silicic crust. *Scientific reports* **7**, 1-8 (2017).
- 864 88. Morriss, M. C., Karlstrom, L., Nasholds, M. W. & Wolff, J. A. The Chief Joseph dike swarm  
865 of the Columbia River flood basalts, and the legacy data set of William H. Taubeneck. *Geosphere*  
866 **16**, 1082-1106 (2020).

89. Glisovic, P. & Forte, A. M. On the deep-mantle origin of the Deccan Traps. *Science* **355**, 613-616 (2017).
90. Gli\ysovi\'c Petar & Forte, A. M. Two deep-mantle sources for Paleocene doming and volcanism in the North Atlantic. *Proceedings of the National Academy of Sciences* **116**, 13227-13232 (2019).
91. Saunders, A. D. Two LIPs and two Earth-system crises: the impact of the North Atlantic Igneous Province and the Siberian Traps on the Earth-surface carbon cycle. *Geol. Mag.* **153**, 201-222 (2016).
92. Gladchenko, T. P., Coffin, M. F. & Eldholm, O. Crustal structure of the Ontong Java Plateau: modeling of new gravity and existing seismic data. *Journal of Geophysical Research: Solid Earth* **102**, 22711-22729 (1997).
93. Mittal, T. & Richards, M. A. Volatile degassing from magma chambers as a control on volcanic eruptions. *Journal of Geophysical Research: Solid Earth* **124**, 7869-7901 (2019).
94. Jellinek, A. M. & DePaolo, D. J. A model for the origin of large silicic magma chambers: precursors of caldera-forming eruptions. *Bulletin of Volcanology* **65**, 363-381 (2003).
95. Colón, D. P., Bindeman, I. N. & Gerya, T. V. Understanding the isotopic and chemical evolution of Yellowstone hot spot magmatism using magmatic-thermomechanical modeling. *J. Volcanol. Geotherm. Res.* **370**, 13-30 (2019).
96. Huber, C., Townsend, M., Degruyter, W. & Bachmann, O. Optimal depth of subvolcanic magma chamber growth controlled by volatiles and crust rheology. *Nature Geoscience* **12**, 762-768 (2019).
97. Perry-Houts, J. & Karlstrom, L. Anisotropic viscosity and time-evolving lithospheric instabilities due to aligned igneous intrusions. *Geophysical Journal International* **216**, 794-802 (2019).
98. Keller, T., May, D. A. & Kaus, B. J. Numerical modelling of magma dynamics coupled to tectonic deformation of lithosphere and crust. *Geophysical Journal International* **195**, 1406-1442 (2013).
99. Petford, N. Rheology of granitic magmas during ascent and emplacement. *Annu. Rev. Earth Planet. Sci.* **31**, 399-427 (2003).
100. Karlstrom, L., Paterson, S. R. & Jellinek, A. M. A reverse energy cascade for crustal magma transport. *Nature Geoscience* **10**, 604-608 (2017).
101. Magee, C., Ernst, R. E., Muirhead, J., Phillips, T. & Jackson, C. A. in Magma transport pathways in large igneous provinces: lessons from combining field observations and seismic reflection data *Dyke Swarms of the World: A Modern Perspective* 45-85 (Springer, 2019).
102. Wolff, J., Ramos, F., Hart, G., Patterson, J. & Brandon, A. Columbia River flood basalts from a centralized crustal magmatic system. *Nature geoscience* **1**, 177-180 (2008).

- 903 103. Muirhead, J. D., Airoidi, G., Rowland, J. V. & White, J. D. Interconnected sills and inclined  
904 sheet intrusions control shallow magma transport in the Ferrar large igneous province, Antarctica.  
905 *Bulletin* **124**, 162-180 (2012).
- 906 104. Muirhead, J. D., Airoidi, G., White, J. D. & Rowland, J. V. Cracking the lid: Sill-fed dikes  
907 are the likely feeders of flood basalt eruptions. *Earth Planet. Sci. Lett.* **406**, 187-197 (2014).
- 908 105. Block, K. A., Steiner, J. C., Puffer, J. H., Jones, K. M. & Goldstein, S. L. Evolution of late  
909 stage differentiates in the Palisades Sill, New York and New Jersey. *Lithos* **230**, 121-132 (2015).
- 910 106. Reidel, S. P. & Tolan, T. L. Eruption and emplacement of flood basalt: An example from the  
911 large-volume Teepee Butte Member, Columbia River Basalt Group. *Geological Society of*  
912 *America Bulletin* **104**, 1650-1671 (1992).
- 913 107. Parfitt, E. & Head, J. Buffered and unbuffered dike emplacement on Earth and Venus:  
914 Implications for magma reservoir size, depth, and rate of magma replenishment. *Earth, Moon,*  
915 *and Planets* **61**, 249-281 (1993).
- 916 108. Arndt, N., Chauvel, C., Czamanske, G. & Fedorenko, V. Two mantle sources, two plumbing  
917 systems: tholeiitic and alkaline magmatism of the Maymecha River basin, Siberian flood volcanic  
918 province. *Contributions to Mineralogy and Petrology* **133**, 297-313 (1998).
- 919 109. Dessai, A., Markwick, A., Vaselli, O. & Downes, H. Granulite and pyroxenite xenoliths  
920 from the Deccan Trap: insight into the nature and composition of the lower lithosphere beneath  
921 cratonic India. *Lithos* **78**, 263-290 (2004).
- 922 110. Friedrich, A. M. *et al.* Stratigraphic framework for the plume mode of mantle convection  
923 and the analysis of interregional unconformities on geological maps. *Gondwana Research* **53**,  
924 159-188 (2018).
- 925 111. Krob, F. C., Glasmacher, U. A., Bunge, H., Friedrich, A. M. & Hackspacher, P. C.  
926 Application of stratigraphic frameworks and thermochronological data on the Mesozoic SW  
927 Gondwana intraplate environment to retrieve the Paraná-Etendeka plume movement. *Gondwana*  
928 *Research* **84**, 81-110 (2020).
- 929 112. Lin, S. & van Keken, P. E. Multiple volcanic episodes of flood basalts caused by  
930 thermochemical mantle plumes. *Nature* **436**, 250-252 (2005).
- 931 113. Burov, E. & Gerya, T. Asymmetric three-dimensional topography over mantle plumes.  
932 *Nature* **513**, 85-89 (2014).
- 933 114. Leng, W. & Zhong, S. Surface subsidence caused by mantle plumes and volcanic loading in  
934 large igneous provinces. *Earth Planet. Sci. Lett.* **291**, 207-214 (2010).
- 935 115. McQuarrie, N. & Rodgers, D. W. Subsidence of a volcanic basin by flexure and lower  
936 crustal flow: The eastern Snake River Plain, Idaho. *Tectonics* **17**, 203-220 (1998).
- 937 116. Jones, S. & MacLennan, J. Crustal flow beneath Iceland. *Journal of Geophysical Research:*  
938 *Solid Earth* **110** (2005).

- 939 117. Orellana-Rovirosa, F. & Richards, M. Evidence and models for lower crustal flow beneath  
940 the Gal\apagos platform. *Geochem. Geophys. Geosyst.* **17**, 113-142 (2016).
- 941 118. Zhu, J. *et al.* Weak vertical surface movement caused by the ascent of the Emeishan mantle  
942 anomaly. *Journal of Geophysical Research: Solid Earth* **123**, 1018-1034 (2018).
- 943 119. Courtillot, V., Jaupart, C., Manighetti, I., Tapponnier, P. & Besse, J. On causal links  
944 between flood basalts and continental breakup. *Earth Planet. Sci. Lett.* **166**, 177-195 (1999).
- 945 120. Planke, S., Symonds, P. A., Alvestad, E. & Skogseid, J. Seismic volcanostratigraphy of  
946 large-volume basaltic extrusive complexes on rifted margins. *Journal of Geophysical Research:*  
947 *Solid Earth* **105**, 19335-19351 (2000).
- 948 121. Hooper, P. R. The timing of crustal extension and the eruption of continental flood basalts.  
949 *Nature* **345**, 246-249 (1990).
- 950 122. Bryan, S. E. & Ferrari, L. Large igneous provinces and silicic large igneous provinces:  
951 Progress in our understanding over the last 25 years. *GSA Bulletin* **125**, 1053-1078 (2013).
- 952 123. Mitchell, R. N. *et al.* The supercontinent cycle. *Nature Reviews Earth & Environment*, 1-17  
953 (2021).
- 954 124. Vanderkluyzen, L., Mahoney, J. J., Hooper, P. R., Sheth, H. C. & Ray, R. The feeder system  
955 of the Deccan Traps (India): insights from dike geochemistry. *J. Petrol.* **52**, 315-343 (2011).
- 956 125. Bindeman, I. *et al.* pervasive Hydrothermal events Associated with Large igneous provinces  
957 Documented by the columbia River Basaltic province. *Scientific reports* **10**, 1-9 (2020).
- 958 126. Park, Y., Swanson-Hysell, N. L., Lisiecki, L. E. & Macdonald, F. A. Evaluating the  
959 relationship between the area and latitude of large igneous provinces and Earth's long-term  
960 climate state. *Large igneous provinces: A driver of global environmental and biotic changes*,  
961 153-168 (2021).
- 962 127. Dessert, C., Dupré, B., Gaillardet, J., François, L. M. & Allegre, C. J. Basalt weathering laws  
963 and the impact of basalt weathering on the global carbon cycle. *Chem. Geol.* **202**, 257-273  
964 (2003).
- 965 128. Alt, J. C. & Teagle, D. A. The uptake of carbon during alteration of ocean crust. *Geochim.*  
966 *Cosmochim. Acta* **63**, 1527-1535 (1999).
- 967 129. Fitton, J. G. & Godard, M. Origin and evolution of magmas on the Ontong Java Plateau.  
968 *Geological Society, London, Special Publications* **229**, 151-178 (2004).
- 969 130. Neal, C., Mahoney, J. & CHAZEY III, W. Mantle sources and the highly variable role of  
970 continental lithosphere in basalt petrogenesis of the Kerguelen Plateau and Broken Ridge LIP:  
971 Results from ODP Leg 183. *J. Petrol.* **43**, 1177-1205 (2002).
- 972 131. Black, B., Mittal, T., Lingo, F., Walowski, K. & Hernandez, A. Assessing the Environmental  
973 Consequences of the Generation and Alteration of Mafic Volcaniclastic Deposits During Large

974 Igneous Province Emplacement. *Large Igneous Provinces: A Driver of Global Environmental*  
975 *and Biotic Changes*, 117-131 (2020).

976 132. Taylor Jr, H. P. & Forester, R. W. An oxygen and hydrogen isotope study of the Skaergaard  
977 intrusion and its country rocks: a description of a 55 my old fossil hydrothermal system. *J. Petrol.*  
978 **20**, 355-419 (1979).

979 133. Wotzlaw, J., Bindeman, I. N., Schaltegger, U., Brooks, C. K. & Naslund, H. R. High-  
980 resolution insights into episodes of crystallization, hydrothermal alteration and remelting in the  
981 Skaergaard intrusive complex. *Earth Planet. Sci. Lett.* **355**, 199-212 (2012).

982 134. Mittal, T., Self, S. & Jay, A. Thickness characteristics of pāhoehoe lavas in the Deccan  
983 Province, Western Ghats, India, and in continental flood basalt provinces elsewhere. *Frontiers*  
984 *Earth Science-Volcanology*, (Early Access) (2021).

985 135. Reidel, S. P., Camp, V. E., Tolan, T. L. & Martin, B. S. The Columbia River flood basalt  
986 province: Stratigraphy, areal extent, volume, and physical volcanology. *Geological Society of*  
987 *America Special Papers* **497**, 1-43 (2013).

988 136. Kamo, S. L. *et al.* Rapid eruption of Siberian flood-volcanic rocks and evidence for  
989 coincidence with the Permian-Triassic boundary and mass extinction at 251 Ma. *Earth and*  
990 *Planetary Science Letters* **214**, 75-91 (2003).

991 137. Blackburn, T. J. *et al.* Zircon U-Pb geochronology links the end-Triassic extinction with the  
992 Central Atlantic Magmatic Province. *Science* **340**, 941-945 (2013).

993 138. Kasbohm, J. & Schoene, B. Rapid eruption of the Columbia River flood basalt and  
994 correlation with the mid-Miocene climate optimum. *Science advances* **4**, eaat8223 (2018).

995 139. Kasbohm, J., Schoene, B. & Burgess, S. Radiometric Constraints on the Timing, Tempo,  
996 and Effects of Large Igneous Province Emplacement. *Large Igneous Provinces: A Driver of*  
997 *Global Environmental and Biotic Changes*, 27-82 (2020).

998 140. Burgess, S. D. & Bowring, S. A. High-precision geochronology confirms voluminous  
999 magmatism before, during, and after Earth's most severe extinction. *Science advances* **1**,  
1000 e1500470 (2015).

1001 141. Renne, P. R. *et al.* State shift in Deccan volcanism at the Cretaceous-Paleogene boundary,  
1002 possibly induced by impact. *Science* **350**, 76-78 (2015).

1003 142. Sprain, C. J. *et al.* The eruptive tempo of Deccan volcanism in relation to the Cretaceous-  
1004 Paleogene boundary. *Science* **363**, 866-870 (2019).

1005 143. Schoene, B. *et al.* U-Pb constraints on pulsed eruption of the Deccan Traps across the end-  
1006 Cretaceous mass extinction. *Science* **363**, 862-866 (2019).

1007 144. Dodd, S. C., Mac Niocaill, C. & Muxworthy, A. R. Long duration (> 4 Ma) and steady-state  
1008 volcanic activity in the early Cretaceous Paraná–Etendeka Large Igneous Province: new  
1009 palaeomagnetic data from Namibia. *Earth Planet. Sci. Lett.* **414**, 16-29 (2015).



145. Schoene, B., Eddy, M. P., Keller, C. B. & Samperton, K. M. An evaluation of Deccan Traps eruption rates using geochronologic data. *Geochronology Discussions*, 1-25 (2020).
146. Chenet, A., Fluteau, F., Courtillot, V., Gérard, M. & Subbarao, K. Determination of rapid Deccan eruptions across the Cretaceous-Tertiary boundary using paleomagnetic secular variation: Results from a 1200-m-thick section in the Mahabaleshwar escarpment. *Journal of Geophysical Research: Solid Earth* **113** (2008).
147. Pavlov, V. E. *et al.* Geomagnetic secular variations at the Permian-Triassic boundary and pulsed magmatism during eruption of the Siberian Traps. *Geochem. Geophys. Geosyst.* **20**, 773-791 (2019).
148. Xu, Y., Yang, Z., Tong, Y. & Jing, X. Paleomagnetic secular variation constraints on the rapid eruption of the Emeishan continental flood basalts in southwestern China and northern Vietnam. *Journal of Geophysical Research: Solid Earth* **123**, 2597-2617 (2018).
149. Percival, L. M. E. *et al.* Mercury evidence for pulsed volcanism during the end-Triassic mass extinction. *Proc. Natl. Acad. Sci. U. S. A.* **114**, 7929-7934 (2017).
150. Jones, D. S., Martini, A. M., Fike, D. A. & Kaiho, K. A volcanic trigger for the Late Ordovician mass extinction? Mercury data from south China and Laurentia. *Geology* **45**, 631-634 (2017).
151. Lindström, S. *et al.* Volcanic mercury and mutagenesis in land plants during the end-Triassic mass extinction. *Science advances* **5**, eaaw4018 (2019).
152. Woodruff, L. G., Schulz, K. J., Nicholson, S. W. & Dicken, C. L. Mineral deposits of the Mesoproterozoic Midcontinent Rift System in the Lake Superior region-A space and time classification. *Ore Geology Reviews*, 103716 (2020).
153. Leitch, A. & Davies, G. Mantle plumes and flood basalts- Enhanced melting from plume ascent and an eclogite component. *Journal of Geophysical Research* **106**, 2047-2059 (2001).
154. Jiang, Q., Jourdan, F., Olierook, H. K., Merle, R. E. & Whittaker, J. M. Longest continuously erupting large igneous province driven by plume-ridge interaction. *Geology* (2020).
155. Mahoney, J., Storey, M., Duncan, R., Spencer, K. & Pringle, M. Geochemistry and age of the Ontong Java Plateau. *The Mesozoic Pacific: Geology, Tectonics, and Volcanism, Geophys.Monogr.Ser* **77**, 233-261 (1993).
156. Zhu, D. *et al.* The 132 Ma Comei-Bunbury large igneous province: Remnants identified in present-day southeastern Tibet and southwestern Australia. *Geology* **37**, 583-586 (2009).
157. Yu, X., Lee, C. A., Chen, L. & Zeng, G. Magmatic recharge in continental flood basalts: Insights from the Chifeng igneous province in Inner Mongolia. *Geochem. Geophys. Geosyst.* **16**, 2082-2096 (2015).

158. Heinonen, J. S., Luttinen, A. V., Spera, F. J. & Bohrsen, W. A. Deep open storage and shallow closed transport system for a continental flood basalt sequence revealed with Magma Chamber Simulator. *Contributions to Mineralogy and Petrology* **174**, 1-18 (2019).
159. Schmidt, A. *et al.* Selective environmental stress from sulphur emitted by continental flood basalt eruptions. *Nature Geoscience* (2015).
160. Black, B. A. *et al.* Systemic swings in end-Permian climate from Siberian Traps carbon and sulfur outgassing. *Nature Geoscience* **11**, 949 (2018).
161. Thordarson, T. & Self, S. The Roza Member, Columbia River Basalt Group: A gigantic pahoehoe lava flow field formed by endogenous processes? *Journal of Geophysical Research: Solid Earth* (1978–2012) **103**, 27411-27445 (1998).
162. Fendley, I. M. *et al.* Constraints on the volume and rate of Deccan Traps flood basalt eruptions using a combination of high-resolution terrestrial mercury records and geochemical box models. *Earth Planet. Sci. Lett.* **524**, 115721 (2019).
163. Petcovic, H. L. & Dufek, J. D. Modeling magma flow and cooling in dikes: Implications for emplacement of Columbia River flood basalts. *Journal of Geophysical Research: Solid Earth* **110** (2005).
164. Karlstrom, L., Murray, K. E. & Reiners, P. W. Bayesian Markov-Chain Monte Carlo inversion of low-temperature thermochronology around two 8– 10 m wide Columbia River flood basalt dikes. *Frontiers in Earth Science* **7**, 90 (2019).
165. Ghosh, P., Sayeed, M., Islam, R. & Hundekari, S. Inter-basaltic clay (bole bed) horizons from Deccan traps of India: implications for palaeo-weathering and palaeo-climate during Deccan volcanism. *Palaeogeogr. , Palaeoclimatol. , Palaeoecol.* **242**, 90-109 (2006).
166. Olsen, P. E., Kent, D. V., Cornet, B., Witte, W. K. & Schlische, R. W. High-resolution stratigraphy of the Newark rift basin (early Mesozoic, eastern North America). *Geological society of america Bulletin* **108**, 40-77 (1996).
167. Schaller, M. F., Wright, J. D. & Kent, D. V. Atmospheric PCO(2) perturbations associated with the Central Atlantic Magmatic Province. *Science* **331**, 1404-1409 (2011).
168. Sharma, M. Siberian traps. *Geophysical Monograph-AGU* **100**, 273-296 (1997).
169. Sawlan, M. G. Alteration, mass analysis, and magmatic compositions of the Sentinel Bluffs Member, Columbia River flood basalt province. *Geosphere* **14**, 286-303 (2018).
170. Ravizza, G. & Peucker-Ehrenbrink, B. Chemostratigraphic evidence of Deccan volcanism from the marine osmium isotope record. *Science* **302**, 1392-1395 (2003).
171. Xu, J., Suzuki, K., Xu, Y., Mei, H. & Li, J. Os, Pb, and Nd isotope geochemistry of the Permian Emeishan continental flood basalts: insights into the source of a large igneous province. *Geochim. Cosmochim. Acta* **71**, 2104-2119 (2007).



172. Fedorenko, V. A. & Czamanske, G. K. Results of new field and geochemical studies of the volcanic and intrusive rocks of the Maymecha-Kotuy area, Siberian flood-basalt province, Russia. *International Geology Review* **39**, 479-531 (1997).
173. Sheth, H. C., Pande, K. & Bhutani, R. <sup>40</sup>Ar-<sup>39</sup>Ar ages of Bombay trachytes: Evidence for a Palaeocene phase of Deccan volcanism. *Geophys. Res. Lett.* **28**, 3513-3516 (2001).
174. Moore, N., Grunder, A. & Bohrsen, W. The three-stage petrochemical evolution of the Steens Basalt (southeast Oregon, USA) compared to large igneous provinces and layered mafic intrusions. *Geosphere* **14**, 2505-2532 (2018).
175. Bennett, E. N., Lissenberg, C. J. & Cashman, K. V. The significance of plagioclase textures in mid-ocean ridge basalt (Gakkel Ridge, Arctic Ocean). *Contributions to Mineralogy and Petrology* **174**, 1-22 (2019).
176. Reidel, S. P. *et al.* The Grande Ronde Basalt, Columbia River Basalt Group; Stratigraphic descriptions and correlations in Washington, Oregon, and Idaho. *Geological Society of America Special Paper* **239**, 21-53 (1989).
177. Durand, S. R. & Sen, G. Preeruption history of the Grande Ronde formation lavas, Columbia River basalt group, American northwest: evidence from phenocrysts. *Geology* **32**, 293-296 (2004).
178. Ramos, F. C., Wolff, J. A. & Tollstrup, D. L. Sr isotope disequilibrium in Columbia River flood basalts: Evidence for rapid shallow-level open-system processes. *Geology* **33**, 457-460 (2005).
179. Borges, M. R., Sen, G., Hart, G. L., Wolff, J. A. & Chandrasekharam, D. Plagioclase as recorder of magma chamber processes in the Deccan Traps: Sr-isotope zoning and implications for Deccan eruptive event. *Journal of Asian Earth Sciences* **84**, 95-101 (2014).
180. Bryan, S. E. *et al.* The largest volcanic eruptions on Earth. *Earth-Sci. Rev.* **102**, 207-229 (2010).
181. Streck, M. J., Ferns, M. L. & McIntosh, W. Large, persistent rhyolitic magma reservoirs above Columbia River Basalt storage sites: The Dinner Creek Tuff eruptive center, eastern Oregon. *Geosphere* **11**, 226-235 (2015).
182. Rocha, B. C. *et al.* Rapid eruption of silicic magmas from the Paran\'a magmatic province (Brazil) did not trigger the Valanginian event. *Geology* **48**, 1174-1178 (2020).
183. Basu, A. R. *et al.* Widespread silicic and alkaline magmatism synchronous with the Deccan Traps flood basalts, India. *Earth Planet. Sci. Lett.* **552**, 116616 (2020).
184. Peate, D. W. Global dispersal of Pb by large-volume silicic eruptions in the Paraná-Etendeka large igneous province. *Geology* **37**, 1071-1074 (2009).

185. Cather, S. M., Dunbar, N. W., McDowell, F. W., McIntosh, W. C. & Scholle, P. A. Climate forcing by iron fertilization from repeated ignimbrite eruptions: The icehouse–silicic large igneous province (SLIP) hypothesis. *Geosphere* **5**, 315-324 (2009).
186. Tabazadeh, A. & Turco, R. P. STRATOSPHERIC CHLORINE INJECTION BY VOLCANIC-ERUPTIONS - HCI SCAVENGING AND IMPLICATIONS FOR OZONE. *Science* **260**, 1082-1086 (1993).
187. Glaze, L., Self, S., Schmidt, A. & Hunter, S. Assessing eruption column height in ancient flood basalt eruptions. *Earth and Planetary Science Letters* (2014).
188. Thordarson, T. & Self, S. The Laki (Skaftár Fires) and Grímsvötn eruptions in 1783–1785. *Bulletin of Volcanology* **55**, 233-263 (1993).
189. Thordarson, T., Larsen, G., Steinthorsson, S. & Self, S. The 1783–1785 AD Laki-Grímsvötn eruptions II: Appraisal based on contemporary accounts. *Jökull* **53**, 11-47 (2003).
190. Hon, K., Kauahikaua, J., Denlinger, R. & Mackay, K. Emplacement and inflation of pahoehoe sheet flows: Observations and measurements of active lava flows on Kilauea Volcano, Hawaii. *Geological Society of America Bulletin* **106**, 351-370 (1994).
191. Swanson, D. A., Wright, T., Hooper, P. & Bentley, R. *Revisions in stratigraphic nomenclature of the Columbia River Basalt Group* (1979).
192. Brown, R. J., Blake, S., Thordarson, T. & Self, S. Pyroclastic edifices record vigorous lava fountains during the emplacement of a flood basalt flow field, Roza Member, Columbia River Basalt Province, USA. *Geological Society of America Bulletin*, B30857. 1 (2014).
193. Jones, T. J. & Llewellyn, E. W. Convective tipping point initiates localization of basaltic fissure eruptions. *Earth Planet. Sci. Lett.* **553**, 116637 (2021).
194. Wei, Z., Qin, Z. & Suckale, J. Magma mixing during conduit flow is reflected in melt-inclusion data from persistently degassing volcanoes. *Earth and Space Science Open Archive ESSOAr* (2021).
195. Burgisser, A., Bergantz, G. W. & Breidenthal, R. E. Addressing complexity in laboratory experiments: the scaling of dilute multiphase flows in magmatic systems. *J. Volcanol. Geotherm. Res.* **141**, 245-265 (2005).
196. Thordarson, T. & Self, S. The Laki (Skaftár Fires) and Grímsvötn eruptions in 1783–1785. *Bulletin of Volcanology* **55**, 233-263 (1993).
197. Witt, T., Walter, T. R., Müller, D., Guðmundsson, M. T. & Schöpa, A. The Relationship Between Lava Fountaining and Vent Morphology for the 2014–2015 Holuhraun Eruption, Iceland, Analyzed by Video Monitoring and Topographic Mapping. *Frontiers in Earth Science* **6**, 235 (2018).
198. Ross, P. S. *et al.* Mafic volcanoclastic deposits in flood basalt provinces: A review. *Journal of Volcanology and Geothermal Research* **145**, 281-314 (2005).

- 1149 199. Thordarson, T. Accretionary-lapilli-bearing pyroclastic rocks at ODP Leg 192 Site 1184: a  
1150 record of subaerial phreatomagmatic eruptions on the Ontong Java Plateau. *Geological Society,*  
1151 *London, Special Publications* **229**, 275-306 (2004).
- 1152 200. Pyle, D. & Mather, T. Halogens in igneous processes and their fluxes to the atmosphere and  
1153 oceans from volcanic activity: A review. *Chem. Geol.* **263**, 110-121 (2009).
- 1154 201. Dasgupta, R. & Hirschmann, M. M. The deep carbon cycle and melting in Earth's interior.  
1155 *Earth Planet. Sci. Lett.* **298**, 1-13 (2010).
- 1156 202. Wieser, P. E., Jenner, F., Edmonds, M., MacLennan, J. & Kunz, B. E. Chalcophile elements  
1157 track the fate of sulfur at Kīlauea Volcano, Hawai'i. *Geochim. Cosmochim. Acta* **282**, 245-275  
1158 (2020).
- 1159 203. Guex, J. *et al.* Thermal erosion of cratonic lithosphere as a potential trigger for mass-  
1160 extinction. *Scientific reports* **6**, 23168 (2016).
- 1161 204. Broadley, M. W., Barry, P. H., Ballentine, C. J., Taylor, L. A. & Burgess, R. End-Permian  
1162 extinction amplified by plume-induced release of recycled lithospheric volatiles. *Nature*  
1163 *Geoscience* **11**, 682-687 (2018).
- 1164 205. Gales, E., Black, B. & Elkins-Tanton, L. T. Carbonatites as a record of the carbon isotope  
1165 composition of large igneous province outgassing. *Earth Planet. Sci. Lett.* **535**, 116076 (2020).
- 1166 206. Liu, J. *et al.* Plume-driven reocratonization of deep continental lithospheric mantle. *Nature*  
1167 **592**, 732-736 (2021).
- 1168 207. Howarth, G. H. *et al.* Superplume metasomatism: evidence from Siberian mantle xenoliths.  
1169 *Lithos* **184**, 209-224 (2014).
- 1170 208. Ernst, R. E., Davies, D. R., Jowitt, S. M. & Campbell, I. When do mantle plumes destroy  
1171 diamonds? *Earth Planet. Sci. Lett.* **502**, 244-252 (2018).
- 1172 209. Svensen, H. *et al.* Siberian gas venting and the end-Permian environmental crisis. *Earth and*  
1173 *Planetary Science Letters* **277**, 490-500 (2009).
- 1174 210. Aarnes, I., Svensen, H., Polteau, S. & Planke, S. Contact metamorphic devolatilization of  
1175 shales in the Karoo Basin, South Africa, and the effects of multiple sill intrusions. *Chem. Geol.*  
1176 **281**, 181-194 (2011).
- 1177 211. Capriolo, M. *et al.* Deep CO<sub>2</sub> in the end-Triassic Central Atlantic Magmatic Province.  
1178 *Nature communications* **11**, 1-11 (2020).
- 1179 212. Hernandez Nava, A. *et al.* Reconciling Early Deccan Traps CO<sub>2</sub> Outgassing and pre-KPB  
1180 Global Climate. *PNAS* (2021).
- 1181 213. Hartley, M. E., MacLennan, J., Edmonds, M. & Thordarson, T. Reconstructing the deep CO  
1182 2 degassing behaviour of large basaltic fissure eruptions. *Earth Planet. Sci. Lett.* **393**, 120-131  
1183 (2014).

214. Moore, L. R. *et al.* Bubbles matter: An assessment of the contribution of vapor bubbles to melt inclusion volatile budgets. *Am. Mineral.* **100**, 806-823 (2015).
215. Rosenthal, A., Hauri, E. & Hirschmann, M. Experimental determination of C, F, and H partitioning between mantle minerals and carbonated basalt, CO<sub>2</sub>/Ba and CO<sub>2</sub>/Nb systematics of partial melting, and the CO<sub>2</sub> contents of basaltic source regions. *Earth Planet. Sci. Lett.* **412**, 77-87 (2015).
216. Workman, R. K., Hauri, E., Hart, S. R., Wang, J. & Blusztajn, J. Volatile and trace elements in basaltic glasses from Samoa: Implications for water distribution in the mantle. *Earth Planet. Sci. Lett.* **241**, 932-951 (2006).
217. Cabato, J. A., Stefano, C. J. & Mukasa, S. B. Volatile concentrations in olivine-hosted melt inclusions from the Columbia River flood basalts and associated lavas of the Oregon Plateau: Implications for magma genesis. *Chem. Geol.* **392**, 59-73 (2015).
218. Ivanov, A. V. *et al.* Volatile concentrations in olivine-hosted melt inclusions from meimechite and melanephelinite lavas of the Siberian Traps Large Igneous Province: Evidence for flux-related high-Ti, high-Mg magmatism. *Chem. Geol.* **483**, 442-462 (2018).
219. Blake, S., Self, S., Sharma, K. & Sephton, S. Sulfur release from the Columbia River Basalts and other flood lava eruptions constrained by a model of sulfide saturation. *Earth Planet. Sci. Lett.* **299**, 328-338 (2010).
220. Caricchi, L., Sheldrake, T. E. & Blundy, J. Modulation of magmatic processes by CO<sub>2</sub> flushing. *Earth Planet. Sci. Lett.* **491**, 160-171 (2018).
221. Black, B. A. & Manga, M. The eruptibility of magmas at Tharsis and Syrtis Major on Mars. *Journal of Geophysical Research: Planets* (2016).
222. Burton, M. R., Sawyer, G. M. & Granieri, D. Deep carbon emissions from volcanoes. *Reviews in Mineralogy and Geochemistry* **75**, 323-354 (2013).
223. Ilyinskaya, Evgenia and Mobbs, Stephen and Burton, Ralph and Burton, Mike and Pardini, Federica and Pfeffer, Melissa Anne and Purvis, Ruth and Lee, James and Bauguitte, Stéphanie and Brooks, Barbara and others. Globally significant CO<sub>2</sub> emissions from Katla, a subglacial volcano in Iceland. *Geophys. Res. Lett.* **45**, 10-332 (2018).
224. McKay, D. I. A., Tyrrell, T., Wilson, P. A. & Foster, G. L. Estimating the impact of the cryptic degassing of Large Igneous Provinces: A mid-Miocene case-study. *Earth Planet. Sci. Lett.* **403**, 254-262 (2014).
225. Gaillard, F., Scaillet, B., Pichavant, M. & Iacono-Marziano, G. The redox geodynamics linking basalts and their mantle sources through space and time. *Chem. Geol.* **418**, 217-233 (2015).
226. Jugo, P. J. Sulfur content at sulfide saturation in oxidized magmas. *Geology* **37**, 415-418 (2009).

227. Zintwana, M. P., Cawthorn, R. G., Ashwal, L. D., Roelofse, F. & Cronwright, H. Mercury in the Bushveld complex, South Africa, and the Skaergaard intrusion, Greenland. *Chem. Geol.* **320**, 147-155 (2012).
228. Le Vaillant, M., Barnes, S. J., Mungall, J. E. & Mungall, E. L. Role of degassing of the Noril'sk nickel deposits in the Permian-Triassic mass extinction event. *Proc. Natl. Acad. Sci. U. S. A.* **114**, 2485-2490 (2017).
229. Macdonald, F. & Wordsworth, R. Initiation of Snowball Earth with volcanic sulfur aerosol emissions. *Geophys. Res. Lett.* **44**, 1938-1946 (2017).
230. Caricchi, L., Townsend, M., Rivalta, E. & Namiki, A. The build-up and triggers of volcanic eruptions. *Nature Reviews Earth & Environment*, 1-19 (2021).
231. Mittal, T. & Richards, M. A. The magmatic architecture of continental flood basalts II: A new conceptual model. (2021).
232. Chenet, A. *et al.* Determination of rapid Deccan eruptions across the Cretaceous-Tertiary boundary using paleomagnetic secular variation: 2. Constraints from analysis of eight new sections and synthesis for a 3500-m-thick composite section. *Journal of Geophysical Research: Solid Earth (1978–2012)* **114** (2009).
233. Braunger, S. *et al.* Do carbonatites and alkaline rocks reflect variable redox conditions in their upper mantle source? *Earth Planet. Sci. Lett.* **533**, 116041 (2020).
234. Reichow, M. K. *et al.* The timing and extent of the eruption of the Siberian Traps large igneous province: Implications for the end-Permian environmental crisis. *Earth and Planetary Science Letters* **277**, 9-20 (2009).
235. Nielsen, T. F. The shape and volume of the Skaergaard intrusion, Greenland: implications for mass balance and bulk composition. *J. Petrol.* **45**, 507-530 (2004).
236. Bürgmann, R. & Dresen, G. Rheology of the lower crust and upper mantle: Evidence from rock mechanics, geodesy, and field observations. *Annu. Rev. Earth Planet. Sci.* **36**, 531 (2008).
237. Caprarelli, G. & Reidel, S. P. Physical evolution of Grande Ronde Basalt magmas, Columbia River Basalt Group, north-western USA. *Mineralogy and Petrology* **80**, 1-25 (2004).
238. Caprarelli, G. & Reidel, S. P. A clinopyroxene–basalt geothermobarometry perspective of Columbia Plateau (NW-USA) Miocene magmatism. *Terra Nova* **17**, 265-277 (2005).
239. Hartley, M. & Thordarson, T. Melt segregations in a Columbia River Basalt lava flow: a possible mechanism for the formation of highly evolved mafic magmas. *Lithos* **112**, 434-446 (2009).
240. Tao, Y., Putirka, K., Hu, R. & Li, C. The magma plumbing system of the Emeishan large igneous province and its role in basaltic magma differentiation in a continental setting. *Am. Mineral.* **100**, 2509-2517 (2015).

241. Putirka, K. D. Thermometers and barometers for volcanic systems. *Reviews in Mineralogy and Geochemistry* **69**, 61-120 (2008).
242. Black, B. A., Elkins-Tanton, L. T., Rowe, M. C. & Peate, I. U. Magnitude and consequences of volatile release from the Siberian Traps. *Earth and Planetary Science Letters* **317–318**, 363-373 (2012).
243. Liu, Z. *et al.* Unusually thickened crust beneath the Emeishan large igneous province detected by virtual deep seismic sounding. *Tectonophysics* **721**, 387-394 (2017).
244. Cherepanova, Y., Artemieva, I. M., Thybo, H. & Chemia, Z. Crustal structure of the Siberian craton and the West Siberian basin: An appraisal of existing seismic data. *Tectonophysics* **609**, 154-183 (2013).
245. Wolff, J. *et al.* Source materials for the main phase of the Columbia River Basalt Group: Geochemical evidence and implications for magma storage and transport. *The Columbia River Flood Basalt Province: Geological Society of America Special Paper* **497**, 273-291 (2013).
246. Barry, T. *et al.* Eruption chronology of the Columbia River Basalt Group. *Geological Society of America Special Papers* **497**, 45-66 (2013).
247. Thordarson, T. & Höskuldsson, Á. Postglacial volcanism in Iceland. *Jökull* **58**, e228 (2008).
248. Neal, Christina A and Brantley, SR and Antolik, Loren and Babb, JL and Burgess, M and Calles, K and Cappos, M and Chang, JC and Conway, S and Desmither, L and others. The 2018 rift eruption and summit collapse of Kilauea Volcano. *Science* **363**, 367-374 (2019).
249. Lipman, P. W. & Calvert, A. T. Modeling volcano growth on the Island of Hawaii: Deep-water perspectives. *Geosphere* **9**, 1348-1383 (2013).
250. Storey, M., Duncan, R. A. & Tegner, C. Timing and duration of volcanism in the North Atlantic Igneous Province: Implications for geodynamics and links to the Iceland hotspot. *Chem. Geol.* **241**, 264-281 (2007).
251. Matthews, S., Shorttle, O., Rudge, J. F. & MacLennan, J. Constraining mantle carbon: CO<sub>2</sub>-trace element systematics in basalts and the roles of magma mixing and degassing. *Earth Planet. Sci. Lett.* **480**, 1-14 (2017).
252. Self, S., Widdowson, M., Thordarson, T. & Jay, A. E. Volatile fluxes during flood basalt eruptions and potential effects on the global environment: A Deccan perspective. *Earth Planet. Sci. Lett.* **248**, 518-532 (2006).
253. Callegaro, S. *et al.* Microanalyses link sulfur from large igneous provinces and Mesozoic mass extinctions. *Geology* **42**, 895-898 (2014).
254. Saal, A. E., Hauri, E. H., Langmuir, C. H. & Perfit, M. R. Vapour undersaturation in primitive mid-ocean-ridge basalt and the volatile content of Earth's upper mantle. *Nature* **419**, 451-455 (2002).



- 1290 255. Sibik, S., Edmonds, M., MacLennan, J. & Svensen, H. Magmas erupted during the main  
1291 pulse of Siberian Traps volcanism were volatile-poor. *J. Petrol.* **56**, 2089-2116 (2015).
- 1292 256. Sobolev, A., Krivolutsкая, N. & Kuzmin, D. Petrology of the parental melts and mantle  
1293 sources of Siberian trap magmatism. *Petrology* **17**, 253-286 (2009).
- 1294 257. Black, B. A., Hauri, E. H., Elkins-Tanton, L. T. & Brown, S. M. Sulfur isotopic evidence for  
1295 sources of volatiles in Siberian Traps magmas. *Earth Planet. Sci. Lett.* **394**, 58-69 (2014).
- 1296 258. Black, B. A., Elkins-Tanton, L. T., Rowe, M. C. & Peate, I. U. Magnitude and consequences  
1297 of volatile release from the Siberian Traps. *Earth Planet. Sci. Lett.* **317**, 363-373 (2012).
- 1298 259. Self, S., Blake, S., Sharma, K., Widdowson, M. & Sephton, S. Sulfur and chlorine in late  
1299 Cretaceous Deccan magmas and eruptive gas release. *Science* **319**, 1654-1657 (2008).
- 1300 260. Choudhary, B. R., Santosh, M., De Vivo, B., Jadhav, G. & Babu, E. Melt inclusion evidence  
1301 for mantle heterogeneity and magma degassing in the Deccan large Igneous Province, India.  
1302 *Lithos* **346**, 105135 (2019).
- 1303 261. Davis, K. N., Wolff, J. A., Rowe, M. C. & Neill, O. K. Sulfur release from main-phase  
1304 Columbia River Basalt eruptions. *Geology* **45**, 1043-1046 (2017).
- 1305 262. Zhang, Y., Ren, Z. & Xu, Y. Sulfur in olivine-hosted melt inclusions from the Emeishan  
1306 picrites: Implications for S degassing and its impact on environment. *Journal of Geophysical*  
1307 *Research: Solid Earth* **118**, 4063-4070 (2013).
- 1308 263. Marks, L. *et al.* F, Cl, and S concentrations in olivine-hosted melt inclusions from mafic  
1309 dikes in NW Namibia and implications for the environmental impact of the Paraná–Etendeka  
1310 Large Igneous Province. *Earth Planet. Sci. Lett.* **392**, 39-49 (2014).
- 1311 264. Peate, D. W., Peate, I. U., Rowe, M. C., Thompson, J. M. & Kerr, A. C. Petrogenesis of  
1312 high-MgO lavas of the Lower Mull Plateau Group, Scotland: Insights from melt inclusions. *J.*  
1313 *Petrol.* **53**, 1867-1886 (2012).
- 1314 265. Thordarson, T., Self, S., Oskarsson, N. & Hulsebosch, T. Sulfur, chlorine, and fluorine  
1315 degassing and atmospheric loading by the 1783–1784 AD Laki (Skaftár Fires) eruption in  
1316 Iceland. *Bulletin of Volcanology* **58**, 205-225 (1996).
- 1317 266. Clarkson, M. O. *et al.* Ocean acidification and the Permo-Triassic mass extinction. *Science*  
1318 **348**, 229-232 (2015).

## Acknowledgments

T.A.M. acknowledges funding from ERC consolidator grant (ERC-2018-COG-818717-V-ECHO).  
B.A.B. acknowledges funding from NSF EAR 1615147. L.K. acknowledges funding from NSF  
EAR 1848554.

## Author contributions

All authors participated in drafting and revising the article. BAB and TAM led the discussion  
of volatiles and created the volatile compilation, LK led the discussion of formation- and  
member-level tempo, BAB and LK led the discussion of the structure of LIPs and their  
relationship to other volcanic activity, BAB led the discussion of mantle melt generation.

## Competing interests

The authors declare no competing interests.

## Peer review information

*Nature Reviews Earth & Environment* thanks [Referee#1 name], [Referee#2 name] and the other, anonymous,  
reviewer(s) for their contribution to the peer review of this work.

## Publisher's note

Springer Nature remains neutral with regard to jurisdictional claims in published maps and institutional  
affiliations.

## Supplementary information

Supplementary information is available for this paper at <https://doi.org/10.1038/s415XX-XXX-XXXX-X>

## Data Availability Statement:

Data compilation used in Figure 5 are available in a worksheet as a Supplementary Data file, at  
<https://doi.org/10.1038/s415XX-XXX-XXXX-X>.



## Figures

**Figure 1. Large Igneous Provinces represent Earth's largest magmatic events.** **a|** Cross-section representing the crustal and upper mantle structure of a continental Large Igneous Province (LIP) approximately corresponding to the onset of main phase volcanism, **b|** degassing depths, **c|** areal extent for selected LIP lavas<sup>234</sup>, dikes<sup>88</sup>, magma reservoirs<sup>78, 235</sup>, and possible mantle plume head<sup>17</sup>. Representative thin section images correspond to labeled locations in **a**. **d|** cross-polarized light photomicrograph of early Siberian Traps lava with olivine phenocrysts. **e|** olivine-hosted melt inclusion with vapor bubble from the Deccan Traps. **f|** carbonate-bearing cumulate from the Seiland igneous province. **g|** garnet-bearing mantle xenolith from the Udachnaya kimberlite<sup>207</sup>, which sampled the pre-Siberian Traps continental lithospheric mantle (CLM) revealing a halogen-rich reservoir<sup>204</sup> (Box 1) with uncertain but potentially substantial carbon contents<sup>10, 11</sup>. Panel e, image courtesy of Andres Hernandez Nava. Panel f adapted with permission from ref<sup>79</sup>, Elsevier. Panel g, image courtesy of Geoffrey Howarth.

**Figure 2. Evolution of continental Large Igneous Provinces (LIPs).** Changing melting, storage, and stress conditions from the mantle to the surface and through early, main phase, and late stages of LIP magmatism show how an extensive transcrustal plumbing system develops and wanes. **a, c, e|** Illustrations of changing storage depths (fading grayscale corresponds to magmas emplaced during prior stages) and qualitative lithospheric differential stress (pink curve) vs. depth<sup>236</sup> modified to account for the hypothesized reduction in crustal strength from heating by LIP magmas. **b, d, f|** Magma storage pressures from geophysical constraints and clinopyroxene (cpx) barometry<sup>237-240</sup> (see<sup>241</sup> for a review and equations used to calculate pressures from Siberian Traps cpx-melt compositions<sup>242</sup>). Seismic and gravity data from the Siberian Traps, Columbia River Basalts (CRB), and Emeishan have been interpreted as evidence for dense intrusive bodies at 25-40 km depth<sup>74, 76, 243, 244</sup> (shown as grey shaded boxes because the relative timing of intrusion is not constrained). **g, h, i|** Melting pressure estimates calculated with a major element thermobarometer<sup>57</sup>, using compositional data from the Siberian Traps<sup>53, 61, 172</sup> and CRB<sup>135, 245</sup>. For Siberian Traps, early panels include Ivakinsky, Syverminsky, and Pravoboyarsky formations. For CRB, early panels include Steens and Imnaha formations, and late panels include Saddle Mountains Basalts.

**Figure 3. Stratigraphy of the Columbia River Flood Basalts (CRB).** Detailed eruptive and chemical characterization make the CRB a template for understanding the Large Igneous Province (LIP) life cycle. **a, b|** cumulative erupted volume at the member level (black symbols and lines) and average eruption rate at the formation level (red curves) against time and average cumulative lava thickness, respectively. Note the short time interval of main phase (Grande Ronde formation) eruptions compared to that of the entire province. Classification and volumes come from<sup>135</sup> and<sup>174</sup> (for Steens), while dates come from<sup>138, 139, 246</sup>. **c|** the average lava volume per member in log scale, suggesting substantial time evolution of crust-magma interactions that modulate eruption sizes, beginning during the main phase. **d, f|** geochemical indices that track source variability and crustal interactions of CRB magmas. The relative constancy of early main phase lavas account for nearly 50% of the total CRB eruptive output. Symbols and error bars represent the mean and range of geochemical values (the median number of samples per data point is 30). Geochemical data comes from<sup>135, 174, 245</sup>.

**Figure 4. The tempo of Large Igneous Province (LIP) magmatism varies across multiple timescales.** Shorter-term volcanic fluxes can be orders of magnitude higher than mean volcanic fluxes during the main phase of LIP volcanism. **a|** Shorter-term volcanic fluxes are represented as

the volume of individual units, members, or formations, divided by their respective emplacement timescales<sup>138, 139, 143, 146, 164, 176</sup>. Equivalent short-term and long-term fluxes imply steady volcanism (1:1 line). Episodes of short-term eruption rates much higher than long-term fluxes imply volcanic pulses. Intervals with lower volcanic fluxes than long-term rates imply storage or intrusion. At the scale of individual units or members, episodes of high flux likely reflect crustal magma transport. At the scale of formations, changes in mantle melting likely contribute to variations in volcanic flux. Deccan DG6 is a paleomagnetic directional group<sup>232</sup>. Historic and modern episodes of volcanism are shown in (a) for comparison: Laki (15.1 km<sup>3</sup> over 8 months<sup>196</sup> vs. postglacial Iceland-wide average of 0.05±0.01 km<sup>3</sup> year<sup>-1</sup>, Ref. <sup>247</sup>) and Kīlauea (0.8 km<sup>3</sup> over 3 months in 2018<sup>248</sup> and 4.4 km<sup>3</sup> spanning the ~35-year Pu‘u ‘Ō‘ō eruption versus mean Kīlauea volcanic flux<sup>249</sup>). Circles represent LIP eruptions and triangles represent historical analogs. Error bars reflect the range in estimates of duration and volume. b| mean volcanic fluxes during the main phase of LIP volcanism are calculated as the volume divided by geochronologically determined duration<sup>67, 139, 140, 142-144, 250</sup>.

**Figure 5. Melt inclusion and proxy data track CO<sub>2</sub>, S, and halogen budgets in Large Igneous Province (LIP) magmas.** Evolving volatile fluxes during the LIP-life cycle link magma emplacement with environmental shifts (Box 1). NAIP, Ontong-Java and Emeishan data are plotted by default as main phase because the relative stratigraphies and/or distinctions between early, main, and late phase are unclear. **a|** CO<sub>2</sub> vs LIP phase. An assumed mantle CO<sub>2</sub>/Ba ratio of ~140 from<sup>215, 251</sup> was used to estimate initial, pre-degassing magmatic CO<sub>2</sub> contents. Only samples with MgO>7 wt% were used for this calculation on the assumption that these would have experienced the least fractionation and/or assimilation that could modify Ba. A prior estimate of 0.5 wt% CO<sub>2</sub><sup>252</sup> derives from Icelandic and Hawaiian basalts. **b|** S vs LIP phase. contents are shown from melt inclusions and estimated from melt inclusion FeO<sub>Total</sub><sup>219</sup>. For estimates using sulfur partitioning in clinopyroxene see<sup>253</sup>. **c-d|** Halogens vs LIP phase. **e-f|** Halogens vs K and Nd contents for CRB and OJP. K and Nd have been suggested as proxies for Cl and F owing to similar behavior during partial melting and crystallization but have not been applied to LIP volatile calculations to date (see summary in<sup>200</sup>). However, data from the CRB<sup>217</sup> and OJP<sup>65</sup> suggest there are large uncertainties in these proxies (for comparison, Cl/K of ~0.04–0.15 and F/Nd=21 as suggested for ocean island basalts<sup>216, 254</sup> are shown). Error bars represent the interquartile range. Data compilation is provided in Supplementary Dataset 1, including data from the Siberian Traps<sup>58, 218, 255-258</sup>, Deccan Traps<sup>212, 259, 260</sup>, Ontong-Java Plateau (OJP<sup>65</sup>), Columbia River Basalts (CRB<sup>217, 219, 261</sup>), Emeishan<sup>262</sup>, Etendeka<sup>38, 263</sup>, and North Atlantic Igneous Province (NAIP<sup>264</sup>), and Laki<sup>213, 265</sup> (added to the right of the plots; Laki sulfur and halogen data are mean values).

**Figure 6. Regime diagram tracking Large Igneous Province (LIP) evolution.** The life cycle of LIPs and volcanism in other settings can be understood in terms of thermal and rheological controls of the crust on ascending mantle melts. LIP onset is characterized by high melt flux (compared to rift or arc settings on Earth) into a thermally immature crust, so resulting transport is governed by elastic and/or brittle behavior of host rocks and heat loss to the crust. The LIP main phase is characterized by highest mantle melt fluxes. In continental settings, high magma supply interacts with a weakened crust, resulting in an enhanced ductile response of host rocks around intrusions, larger storage zones, and a more robust trans-crustal magma transport network. Rheological transition to a viscous crust could contribute to <1 Myr typical continental LIP main phase durations<sup>59</sup>. Large volume, prolonged shallow storage necessary to generate silicic caldera-forming eruptions<sup>181</sup> becomes rheologically feasible at this stage of continental LIPs. Waning phases of

LIPs see declining mantle melt flux in a thermally evolved (but cooling) crust, possibly transitioning to a storage-dominated regime. Additional data from oceanic provinces is needed to understand whether and how their life cycle differs from continental LIPs. Figure adapted from Ref <sup>100</sup>, Springer Nature Limited.

## Boxes

### Box 1. Large Igneous Provinces (LIPs) and mass extinctions

There is a well-established correlation between the ages of Phanerozoic LIPs and mass extinction and oceanic anoxic events. These links are substantiated by increasingly high-precision U-Pb and Ar-Ar geochronology of both LIP rocks and environmental perturbations determined from sedimentary records. Gases and particles released from magmas and country rocks during LIP volcanism have been proposed as key candidates for triggering these severe Earth system responses<sup>6-9</sup>. Impacts include: warming and ocean acidification from CO<sub>2</sub> release<sup>266</sup>; acid mist and short-term cooling from sulfur outgassing<sup>159, 160</sup>; and ozone depletion from volcanic and metamorphic halogen compounds<sup>210</sup>. Changes in surface temperature have follow-on consequences for hydrology and ocean circulation<sup>160</sup>. On longer timescales (~1-10 Myr), weathering of LIP basalts can draw down CO<sub>2</sub>, perhaps drastically<sup>127</sup>. However, mechanistic insights into which of these processes are the most critical drivers of ecosystem collapse remains elusive. Earth system modelling employed to test the mechanisms responsible for observed environmental disruption depends on realistic volatile emission scenarios. While constraining such model inputs is challenging for LIPs, new datasets are becoming available that quantify volatile release from different parts of the LIP system (see Table below compiling data for the Siberian Traps). Other key parameters include eruption column height, volcanic versus intrusive flux, and durations of eruptions and hiatuses.

Volatile	Total from Magma <sup>a</sup> (Mt)	Total from Mantle (Mt)	Total from CLM (Mt)	Total from Crust (Mt)	Fluxes <sup>b</sup> (Mt yr <sup>-1</sup> )	Possible consequences
CO <sub>2</sub>	<sup>c</sup> 10 <sup>7</sup> -10 <sup>8</sup>	<sup>d</sup> 1.7 × 10 <sup>8</sup>	?	<sup>e</sup> 10 <sup>8</sup>	10 <sup>2</sup> -10 <sup>4</sup>	Long-term warming, ocean acidification, changes to hydrology and ocean circulation
SO <sub>2</sub>	<sup>f</sup> 12.6–15.6 × 10 <sup>6</sup>	<sup>g</sup> 11.4–14.0 × 10 <sup>6</sup>	?	<sup>g</sup> 10 <sup>6</sup>	10 <sup>1</sup> -10 <sup>3</sup>	Transient cooling, acid mist, changes to hydrology and ocean circulation
Halogens	<sup>f</sup> 3.4–8.7 × 10 <sup>6</sup> HCl, 7.1–13.6 × 10 <sup>6</sup> HF	<sup>d</sup> 1.8 × 10 <sup>7</sup> HCl	<sup>h</sup> 8.7 × 10 <sup>6</sup> HCl, 2.3 × 10 <sup>4</sup> Br, 96 I	?	10 <sup>0</sup> -10 <sup>3</sup> HCl, HF 10 <sup>-2</sup> -10 <sup>0</sup> Br 10 <sup>-4</sup> -10 <sup>-2</sup> I	Ozone depletion (from HCl, HBr, not F); local acidity
CH <sub>4</sub> , organo-halogens, Hg, trace metals	?	?	?	?	?	Warming, ozone depletion, toxicity

1 Mt = 10<sup>12</sup> g. <sup>a</sup>Magma could include contributions from deep mantle, CLM and crust. <sup>b</sup>Fluxes are order-of-magnitude estimates based on magnitudes in preceding columns and assumed outgassing durations of 10<sup>4</sup>-10<sup>6</sup> years. The 10<sup>4</sup>-year duration is motivated by the cumulative duration of intense eruptive episodes assuming magma flux of 10<sup>2</sup> km<sup>3</sup> year<sup>-1</sup>, consistent with paleomagnetic evidence for emplacement of a large portion of the eruptive volume of the Siberian Traps across a cumulative duration of ~10<sup>4</sup> years<sup>147</sup>. <sup>c</sup>From modeling magma transport through carbon-rich upper crustal rocks<sup>82</sup>. <sup>d</sup>From thermomechanical modeling and petrological evidence for recycled oceanic crust<sup>34</sup>. <sup>e</sup>From crustal metamorphism<sup>209</sup>. <sup>f</sup>Based on melt inclusion measurements and 4 × 10<sup>6</sup> km<sup>3</sup> of extrusive rocks<sup>258</sup>. <sup>g</sup>From sulfur isotopes<sup>257</sup>. <sup>h</sup>From xenolith data scaled to HCl flux assuming the CLM flux dominates halogen emissions<sup>204</sup>.

## Glossary

**Mass extinctions** are abrupt losses of biodiversity in which >75% of species vanish over geologically short intervals, yielding extinction rates that far exceed rates at which new species evolve.

**Continental lithospheric mantle (CLM)** is the upper-most part of the mantle that is mechanically attached to continental crust and does not participate in mantle convection.

**Trans-crustal transport** is the suite of processes by which magma ascends through the crust to the surface through a network of storage zones (magma chambers) and dikes and/or sills.

**Mantle melting** occurs when the decompression, temperature, or composition of mantle material (or a combination of these) place it above its solidus—but almost universally below its liquidus, when it would be entirely molten.

**Partial melting** is a fractional degree of melting, from 0% at the solidus to 100% at the liquidus.

**Tholeiitic** basalts are iron-rich basalts like those found at mid-ocean ridges, commonly thought to originate at relatively high (>10%) degrees of melting, typically at pressures <3 GPa.

**Alkaline** basalts are rich in K and Na and are thought to originate at relatively low degrees of melting (<5%), often at pressures >3 GPa.

**Tempo** of magmatism is its pace, for example, how the intensity of magmatic activity varies through time -- it often refers to the volume and frequency of eruptions at the surface.

**Thermochemical mantle plumes** are focused upwellings from the deep mantle with anomalous composition and temperature that cause them to be buoyant.

**Edge-driven convection** invokes lithospheric thickness variations, for example across the edges of continents, to drive local convection and decompression melting.

**Delamination** when the formation of dense eclogites causes the lowermost crust or lithospheric mantle to sink into the underlying mantle.

**Mantle potential temperature** is the temperature of a parcel of mantle if brought adiabatically to Earth's surface, which enables comparison of mantle temperatures from different depths.

**Geodynamic models** solve conservation equations for mass, momentum, and energy to predict how the solid Earth evolves, typically focused on large length and timescales and typically involving mantle convection.

**Major elements** are those with concentrations exceeding ~1 wt %--in this case, within magmas—including Si, Fe, O, Mg, Ca, and Al.

**Trace elements** are those with concentrations typically <1 wt %, such as Rare Earth Elements.

**Magmatic plumbing system** transcrustal magma transport and storage networks that feed surface eruptions.

**Intrusive to Extrusive ratio** is the proportion of primary magma that freezes upon ascent versus the volume that erupts on the surface.

**Mantle xenoliths** are fragments of mantle rock entrained and transported in a magma - the presence of dense xenoliths in erupted volcanic rocks reflects sufficiently rapid ascent to keep them entrained.

**Dynamic topography** is often defined as the time-dependent generation of surface relief from non-isostatic mantle or crustal flow.

**Incompatible trace elements** are strongly enriched in the melt relative to solid phases during mantle melting, often due to ionic charge or radius that hinders their easy substitution into the structure of the solid phases that are present.

**Bulk distribution coefficient** ( $D_i$ ), commonly abbreviated as  $D_i = C_i^{\text{solid}} / C_i^{\text{liq}}$ , for the concentration of a species  $i$  in a solid residue ( $C_i^{\text{solid}}$ ) relative to in the liquid ( $C_i^{\text{liq}}$ ). By definition,  $D_i \ll 1$  for incompatible species.

**Rehomogenization** is experimental reheating of crystals bearing recrystallized melt inclusions until inclusions melt, and then quenching to form homogeneous glass suitable for obtaining representative compositions by microanalysis.

**CO<sub>2</sub> flushing** refers to exsolution of CO<sub>2</sub>-rich fluids at depth in the magmatic system, which then ascend and modify the balance of volatiles in shallower (typically more CO<sub>2</sub>-depleted) magmas.

**Magma redox** refers to the balance between oxidation and reduction that determines the oxidation state of chemical species in the magma.

Fig 1

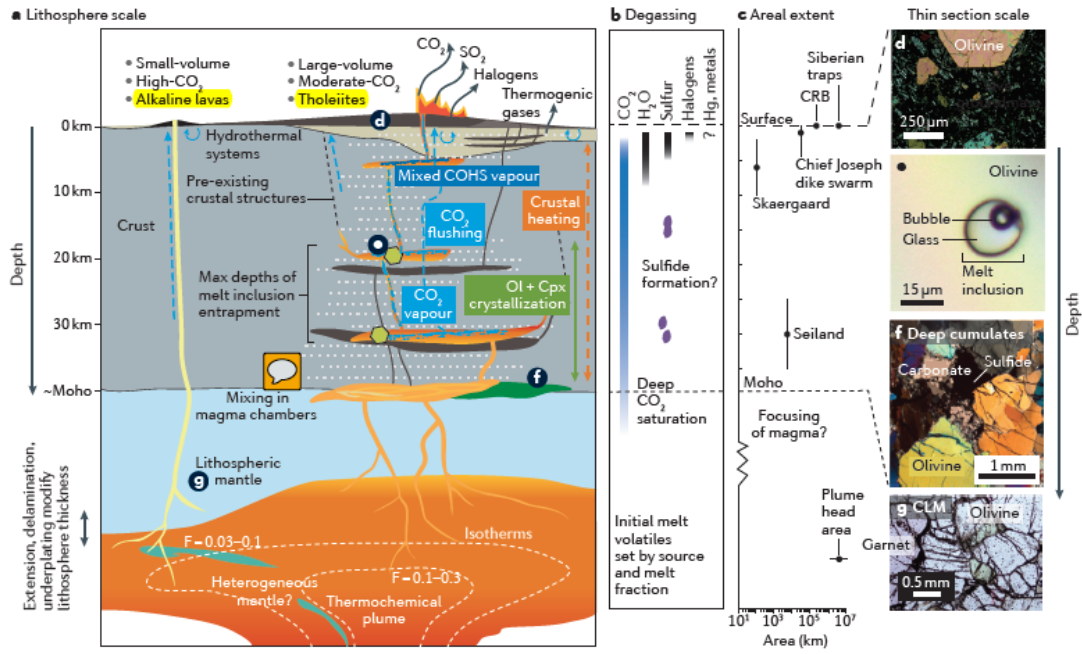


Fig 2

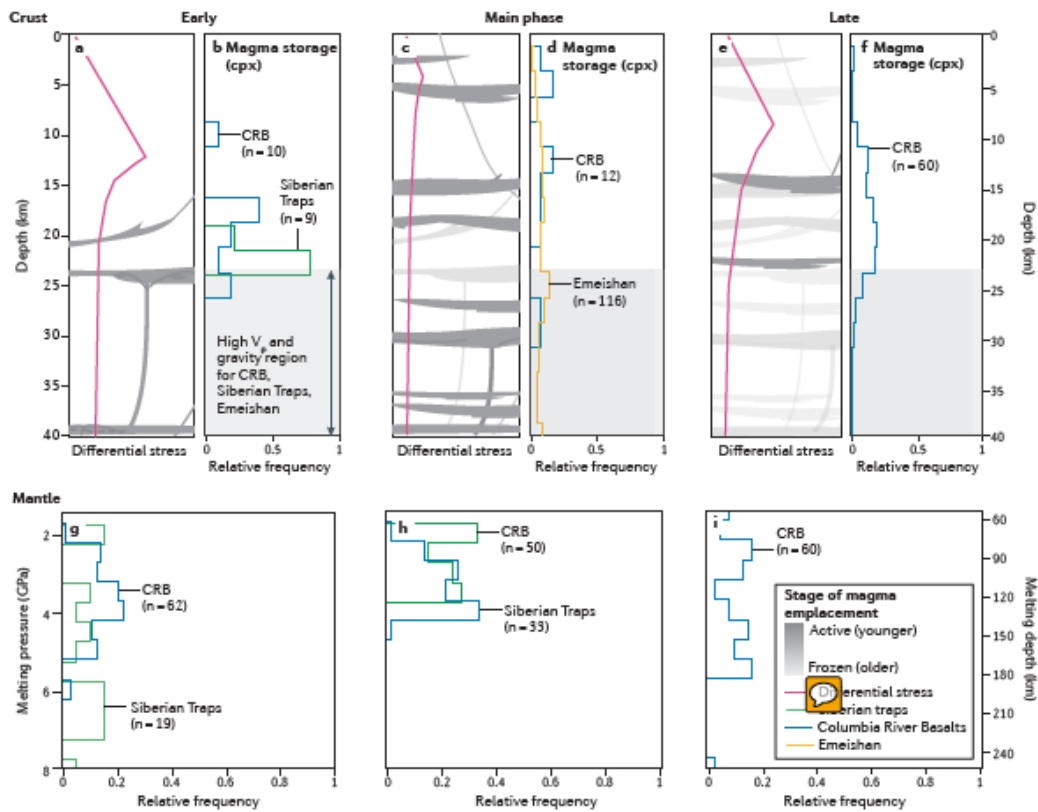




Fig 3

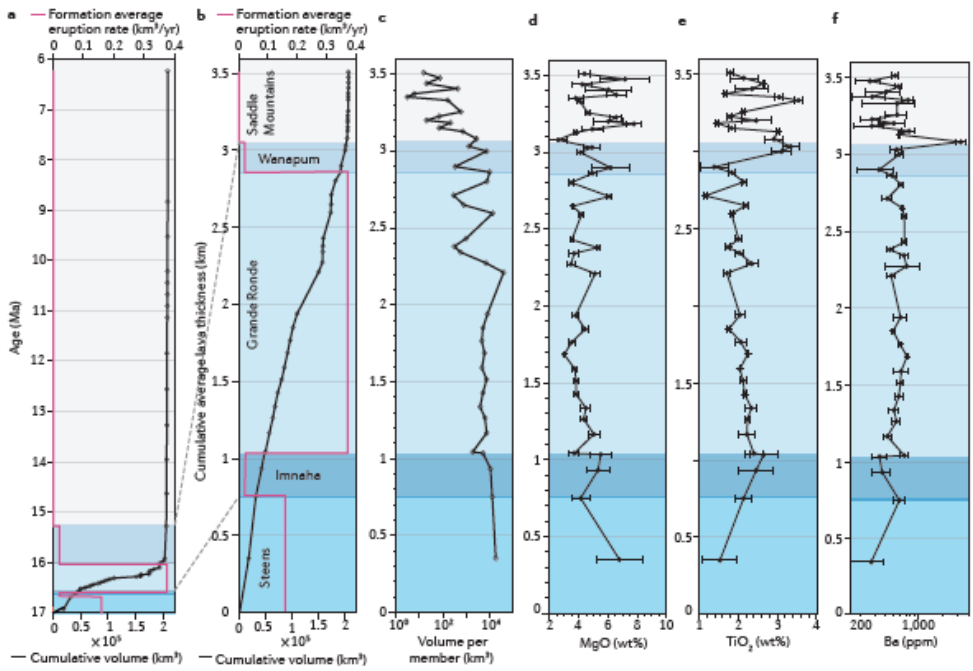


Fig 4

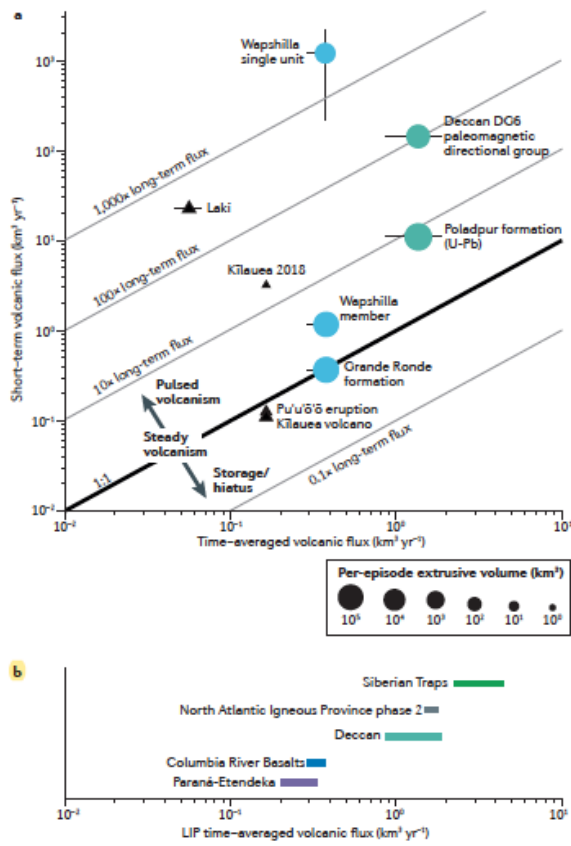


Fig 5

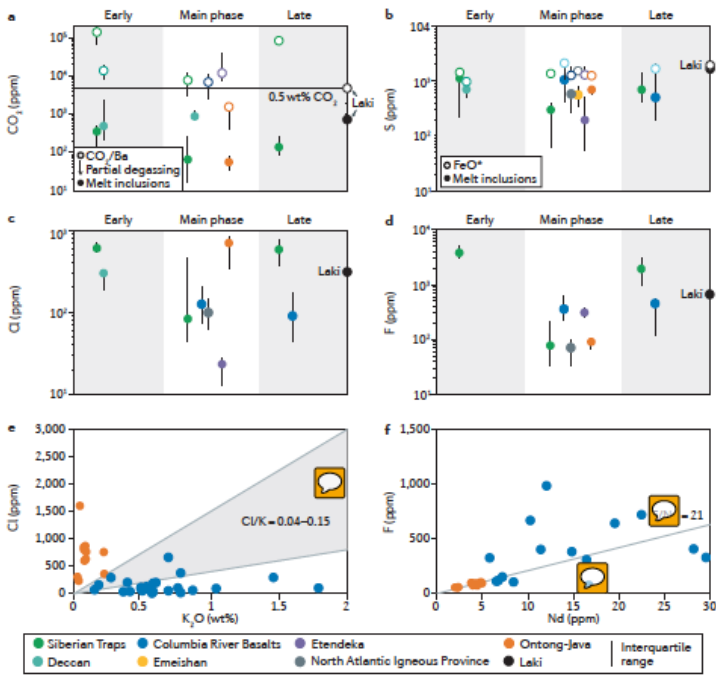


Fig 6

